HERON is jointly edited by:
STEVIN-LABORATORY of the
faculty of Civil Engineering,
Delft University of Technology,
Delft, The Netherlands
and
TNO-INSTITUTE
FOR BUILDING MATERIALS
AND STRUCTURES.
Rijswijk (ZH), The Netherlands
HERON contains contributions
based mainly on research work
performed in these laboratories
on strength of materials, structures
and materials science.

ISSN 0046-7316

Secretary:
G. J. van Alphen
Stevinweg 1
P.O. Box 5048
2600 GA Delft, The Netherlands
Tel. 0031-15-785919
Telex 38070 BITHD

HERON vol. 33
1988
no. 2

Contents

NUMERICAL AND EXPERIMENTAL DETERMINATION OF STRAIN (STRESS) CONCENTRATION FACTORS OF WELDED JOINTS BETWEEN SQUARE HOLLOW SECTIONS

R. S. Puthli
TNO Institute for Building Materials and Structures

J. Wardenier
Delft University of Technology

C. H. M. de Koning
TNO Institute for Building Materials and Structures

A. M. van Wingerde
Delft University of Technology

F. J. van Dooren
Delft University of Technology

Summary 3
Notation 4
1 Introduction and background 5
2 Definitions 6
3 Hot spot strain (stress) range method for fatigue design 9
4 The fatigue design approach for rectangular (square) hollow section joints 10
5 Description of the finite elements used 11
6 Preliminary study to establish basis for numerical modelling 14
7 General approach for determining SNCF values for parametric study 21
7.1 Procedure for experimental work 22
7.2 Procedure for comparison of experiments with numerical modelling 23
7.3 Procedure for numerical analyses of strains and tabulation of strain concentration factors (SNCF) using nominal dimensions 23
7.4 Procedure for making design recommendations 25
8 Study on X joints with axial tension in braces ... 25
9 Study on T joints with axial tension or moment in the brace 34

10 Study on the effect of axial tension and bending in the braces of K joints with gap on the strain concentration factors 36
10.1 Loading and boundary conditions on K joints with gap and no eccentricity of system lines 37
10.2 Implied effect of weld using a shift rule . 38
10.3 Experimental comparison 40
10.4 Parametric study using nominal dimensions of hollow sections 44
11 Concluding remarks 47
12 Acknowledgements 48
13 References 49

Publication in HERON since 1970

Summary

This article presents methods of approach for finite element modelling of joints made of rectangular hollow steel sections where the brace members are welded to the face of the chord, to obtain strain (stress) concentration factors, SNCF (SCF). X, T and K type joints are considered. Simple modelling methods are applied for practical reasons, so that straight-forward use in large scale parametric studies is possible. Details that influence the results due to modelling are discussed. In the range of parameters considered for subsequent parametric studies, a few selected representative joints are considered for experimental comparison. The comparisons between experiments and finite element analyses give confidence in the results. SNCF values at critical locations are determined for a range of preselected geometrical parameters and used in regression analyses to provide parametric SNCF formulae. The SNCF values from these formulae have a good correlation with the values determined from the finite element analyses. The SNCF formulae are also shown graphically to give a visual impression of the influence of the various geometrical parameters on the magnitudes.

Notation

b_0	external width of chord member
b_1	external width of brace member
f_a	axial strain component of nominal strain in K joint
f_b	bending strain component of nominal strain in K joint
t_0	wall thickness of chord member
t_1, t_2	wall thickness of brace members
FE	finite element
N	number of cycles
N_f	number of cycles to failure
R	stress ratio between maximum and minimum nominal stress in a load cycle for constant amplitude fatigue loading
SCF	stress concentration factor
SNCF	strain concentration factor
S_r	stress range or difference between maximum and minimum stress in a load cycle for constant amplitude fatigue loading
$S_{r\,nom}$	nominal stress range
$S_{r\,h.s.}$	hot spot stress range $= S_{r\,nom} \cdot$ SCF
β	brace to chord width ratio b_1/b_0
ε_r	strain range, or difference between maximum and minimum strain in a load cycle for constant amplitude fatigue loading
$\varepsilon_{r\,h.s.}$	hot spot strain range $= \varepsilon_r \cdot$ SNCF
$\varepsilon_{r\,nom}$	nominal strain range
2γ	width of wall to thickness ratio of the chord b_0/t_0
τ	brace to chord wall-thickness ratio t_1/t_0
CIDECT	Comité Internationale pour le Developpement et l'Etude de la Construction Tubulair (International Committee for the Development and Study of Tubular Construction).
ECSC	European Community of Steel and Coal

Numerical and experimental determination of strain (stress) concentration factors of welded joints between square hollow sections

1 Introduction and background

A dominant factor affecting fatigue under cyclic or fluctuating loads is localized stress (or strain) concentration. Under the fluctuating stresses or strains that are induced at these concentration points, progressive localized permanent damage can occur, called fatigue. This may culminate in cracks or complete failure after a sufficient number of fluctuations depending on the stress or strain concentration factor. For statically loaded joints with sufficient deformation capacity, the stress or strain concentration is of minor importance due to stress redistribution by local yielding.
The work described here is considered under linear elastic conditions and only refers to high cycle fatigue. Although, in practice, fluctuating loads occur as constant amplitude or variable amplitude loads, fatigue behaviour is usually investigated on the basis of constant amplitude loading tests (see Fig. 1), and are primarily dependent upon three parameters:

stress range $S_r = \sigma_{max} - \sigma_{min}$;
stress ratio $R = \sigma_{min}/\sigma_{max}$;
thickness of the member undergoing fatigue failure.

Here, σ_{max} = maximum nominal stress in a constant amplitude loading cycle, and
σ_{min} = minimum nominal stress in a constant amplitude loading cycle.

Nominal stress, σ_{max} or σ_{min}, is the stress derived in a member from simple elastic theory. It therefore represents a situation excluding the effects of geometrical discontinuities which cause stress concentration.
The number of cycles to failure decreases with increasing stress range and thickness. The stress ratio may have some influence on small thicknesses. The most significant factor is the stress range, with the stress ratio being less important when residual stresses are present in welded connections. Other factors such as environmental effects can aggravate the situation and also be taken into account.

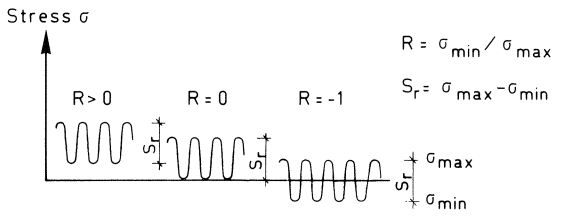

Fig. 1. Stress range S_r and stress ratio R.

In practice, constant amplitude loading is seldom present. Therefore, cumulative damage rules are used to describe the behaviour under spectrum loading. A popular rule, which is no worse than other known rules is the Palmgren-Miner's rule, where fatigue damage accumulates linearly with the number of cycles at a particular load level:

$$\sum \frac{n_i}{N_i} \leq 1$$

where

n_i = number of cycles at load level i
N_i = number of cycles to failure at this load level i

Nowadays, the fatigue strength is generally related to the geometrical hot spot strain (stress). This method requires information about the strain or stress concentration factors (SNCF or SCF respectively). For circular hollow section joints, various parametric formulae are available. For square or rectangular hollow section joints, only limited evidence exists. This is one of the reasons that an European programme has been started, from which the numerical investigations dealt with in this paper are a part. In this article, the numerical determination of SNCFs in square hollow section joints are described. In particular, X and T joints and K joints with gap are considered. Numerical modelling is checked with experiments prior to commencing parametric work.

2 Definitions

The weld toes in welded joints have preformed notches and therefore positions of weakness where fatigue cracks are most likely to occur. In Civil Engineering structures, therefore, attention is primarily focussed on fatigue of welded joints.
The International Institute of Welding (IIW, 1985) has provided recommendations in which certain definitions in relation to fatigue design procedure for hollow section joints are listed. These are given below with small adaptations as a useful reference, which will be used henceforth:

Fatigue
When fluctuating loads are applied to a material they may induce local stresses and strains which are sufficient to induce localised micro-structural changes resulting in the development of cracks. This process is known as fatigue. The cracks, fatigue cracks, can grow to a size sufficient to cause failure.

Fatigue life
The fatigue life is generally specified as the number of cycles N of stress or strain of a specified character, that a given joint sustains, before failure of a specified nature occurs. In the IIW recommendations a crack through the wall is considered as failure.

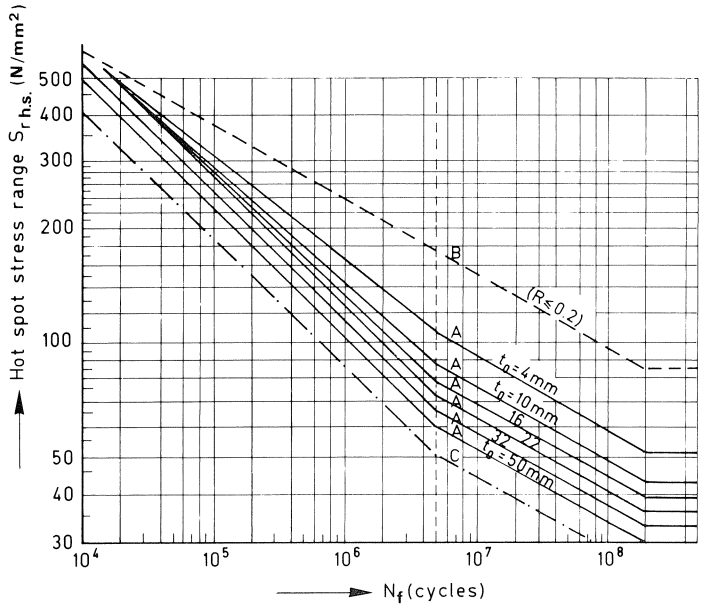

Fig. 2. $S_{r\,h.s.}$-N_f curves for hollow section joints.

S_r-N_f curve

A S_r-N_f curve gives the relationship between the stress range and the number of cycles to failure. Conventionally, the range of stress is plotted on the vertical axis and the number of cycles on the horizontal axis, using logarithmic scales for both axes.

The $S_{r\,h.s.}$-N_f curves given in Fig. 2 for hollow section joints have been derived from a statistical analysis of relevant experimental data and represent lives which are less than the mean life by two standard deviations. It may be noted that later research (Van Delft, et al. 1985) has shown that the thickness effect is larger than that adopted in these recommendations.

Nominal stress

The nominal stress is specified as the maximum stress in a cross-section calculated on the actual cross-section by simple elastic theory, without taking into account the effect of geometrical discontinuities due to the joint configuration on the stress.

Hot spot stress

The stress range to be used for fatigue design of hollow section joints is the range of the "hot spot" stress. The "hot spot" is defined as the point along the weld toe where the extrapolated stress on a line perpendicular to the weld toe has its maximum value. The extrapolation must be carried out from the region outside the influence of the effects of the weld geometry and discontinuties at the weld toe, but close enough to fall inside the zone of the stress gradient caused by the global geometrical effects. The extrapolation is to be carried out on the brace (cut and welded member) side and the chord (continuous member) side of each weld (see Fig. 3).

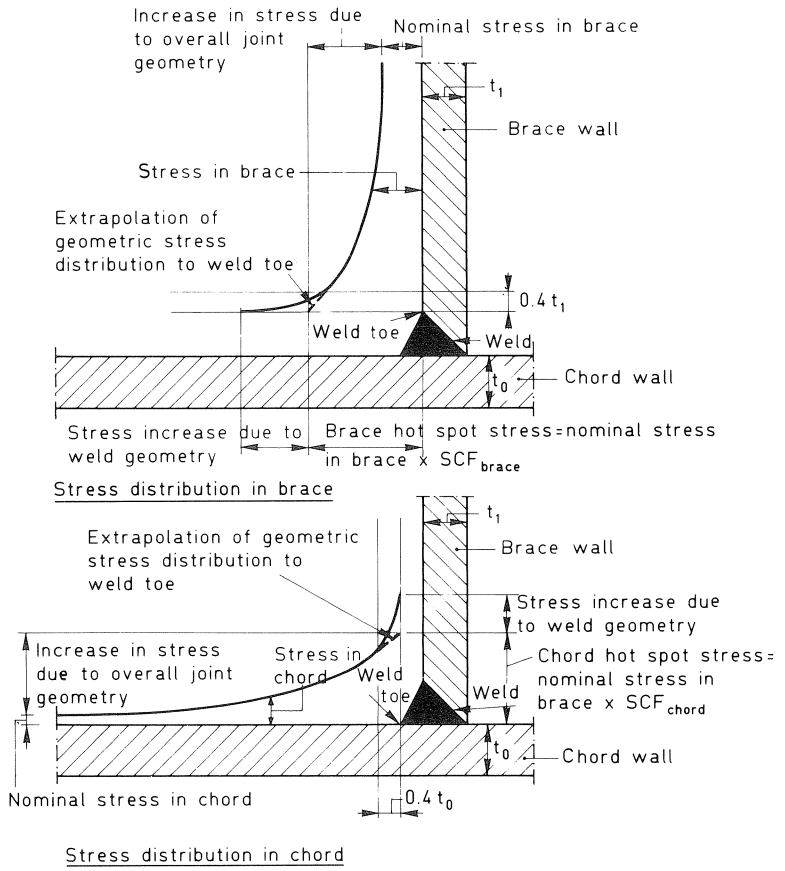

Fig. 3. Hot spot stress definition in nodal joints.

Strain (stress) concentration factor

The strain (stress) concentration factor SNCF (SCF) is defined as the geometrical hot spot strain (stress) divided by the nominal strain (stress) in an attached brace. In joints with more than one brace, each brace has to be considered. Generally, strain (stress) concentration factors are calculated for the chord and brace.

Stress range

The stress range S_r is defined as the algebraic difference between the maximum and minimum stresses in a stress cycle (see Fig. 1). The nominal stress range is based on the nominal stresses while the hot spot stress range is based on hot spot stresses.

Stress ratio R

The stress ratio R is defined as the ratio between the minimum and maximum stresses for constant amplitude loading taking account of the sign of the stress. Tension is taken as positive and compression as negative.

There are several methods used to describe the fatigue behaviour of joints. They can generally be categorized into the hot spot stress (or strain) range based methods as described in Chapter 3, or methods based upon nominal stress (or strain). In the methods based upon nominal stress, the stress concentration is indirectly included by classification of joints into different *S-N* curves, or by including some of the most influential geometric parameters into factors to multiply with the nominal stress or stress level of the *S-N* curves.

3 Hot spot strain (stress) range method for fatigue design

This method relates the geometrical hot spot strain or stress at the fatigue crack of individual joints directly with fatigue failure and therefore has considerable advantages over other methods.In the past twenty years, many international investigations have been carried out on circular hollow section joints, leading to $S_{r\,h.s.}$-N_f curves, together with a number of parametric formulae for determining the stress concentration factors (SCFs) for various types of joints. As an example, Fig. 2 shows the $S_{r\,h.s.}$-N_f curves recommended by IIW SC-XV-E.

The advantage of the hot spot stress method is that all kinds of joints are related to the same $S_{r\,h.s.}$-N_f curves by the stress concentration factors, determined by parametric formulae. However, if parametric formulae do not exist, or the parameters are outside the range of validity of the formulae, expensive numerical analyses or measurements on experiments have to be carried out.

Numerical analyses have the distinct advantage of giving the exact positions, directions and magnitudes of high stresses and the patterns of stress distribution in the entire zone of the specific joint being considered, based upon the amount of refinement put into the modelling. For practical purposes, the modelling will not necessarily give the actual peak stress at the weld toe, due to inherent difficulties in representing the singularity at the notch formed between weld and parent metal. However, since only "geometric stress" is used to define the SCF (see Fig. 3), this information is not necessary.

In an European Offshore Programme, thin shell elements have been used for simple joints in determining SCFs and parametric formulae developed for circular hollow section in-plane girder joints. Reference may also be made to Kuang et al (1977), and Gibstein (1978). Wordsworth (1981, 1987) has provided formulae on the basis of measurements from acrylic model tests.

Van Delft, et al. (1987) have shown that the parametric equations proposed by Efthymiou, et al. (1985) gave good correlation with experimental values. Furthermore, the scatter of test results could be reduced considerably, providing a factor proportional to thickness to the power of 0.4 is adopted in the $\varepsilon_{r\,h.s.} - N_f$ or $S_{r\,h.s.} - N_f$ curves.

Some parametric formulae are only provided for stress concentration factors at the location giving the highest values for a particular single load action. However, for combined loading, the location and value of the stress concentration factors can be different. The appropriate summation of stress concentration factors can only be obtained from those sets of parametric formulae which give sufficient information at several

locations. As may be observed in the present work, a number of locations are considered.
In spite of all the restrictions mentioned above, the hot spot stress (or strain) method has proved to be the most commonly used approach for circular hollow sections.

4 The fatigue design approach for rectangular hollow section joints

For rectangular hollow section joints, only very limited information is available on stress concentration factors (Wardenier, 1982). Because of this, parametric formulae have not been formulated for general determination of SCF values. The "classification method" is presently used in Eurocode 3 for rectangular hollow section joints, where the joints are primarily classified into groups with nearly the same fatigue resistance. The geometrical SCF is indirectly taken into account by having different $S_{r\,h.s.}$-N_f curves for different types of joints.
An ECSC research programme on rectangular hollow section joints, also sponsored by CIDECT, is therefore under way in Germany and the Netherlands, with four participants, namely, Mannesmannröhren-Werke A.G., Düsseldorf, Universität Karlsruhe, Delft University of Technology and TNO Institute for Building Materials and Structures, Rijswijk. The investigation is on X joints, T joints, K joints with gap and K joints with overlap. Fig. 4 gives the types of joints that are considered here, together with the joint parameters. The work on X and T joints is carried out jointly by the Delft University of Technology and TNO-IBBC, while the work on K joints with gap and overlap is carried out at Universität Karlsruhe. Additional work on larger dimensions (twice the scale of the work at Karlsruhe) is being carried out on K joints with gap and overlap by Delft University of Technology and TNO-IBBC. This work is only on strain concentration factors and no fatigue testing is involved. However, only the work on determining the SNCF of K joints with gap, using the larger square hollow sections, will be presented here in order to illustrate the method of approach. This is because the geometry, loading and behaviour of K joints with gap or overlap is radically different from those for X and T joints.
The aim of the above research programme is to provide fatigue design recommendations, where $\varepsilon_{r\,h.s.} - N_f$ curves and SNCF data based upon nondimensional parameters will be given. The research programme for these type of joints consists primarily of an experimental and a numerical part. The experimental part consists of determining the strain concentration factors (SNCFs) at the weld toes from measurements before commencing the fatigue tests and of determining the fatigue life of the specimens. The numerical part consists of determining SNCFs for nominal dimensions of the hollow sections and SNCF formulae from the parametric study.
The methods of approach for the work on square hollow section joints, as well as noteworthy problems encountered and some of the results, are discussed in the remaining of this text. Attention will be solely devoted to the determination of strain concentration factors and establishment of parametric formulae for these joints. For details of fatigue data, reference may be made to reports under preparation for the ECSC. These

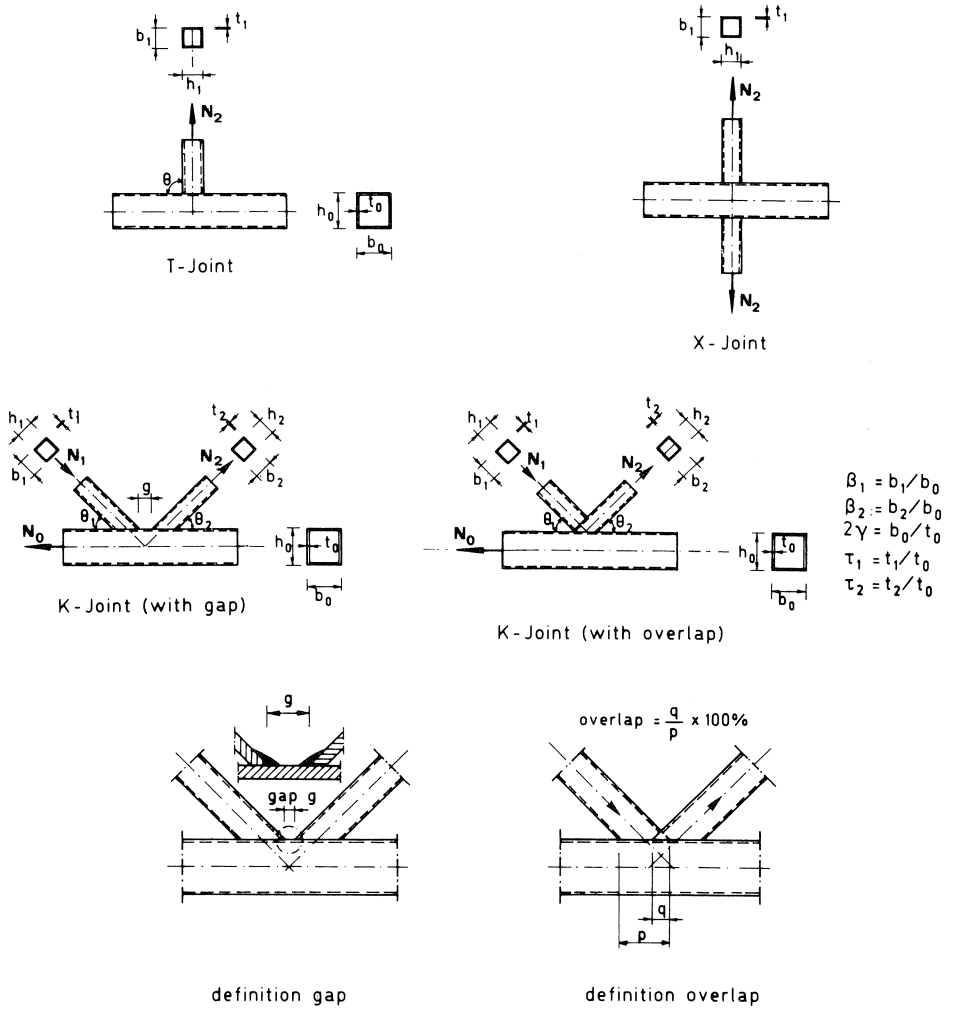

Fig. 4. Basic types of joints and joint parameters investigated.

reports are confidential until the end of the project (1989), when they may be obtained by permission from the ECSC.

5 Description of the finite elements used

The in-house general purpose finite element program DIANA (DIsplacement ANAlyser) is used for all the analytical work (De Borst et al. 1985). Only the linear elastic part is required for this research work. The steel properties used are always with the modulus of elasticity (E) of 210000 N/mm^2 and Poisson's ratio (ν) of 0.3. Several types of elements have been used, namely:

1. 8 noded, 40 degree of freedom thick shell elements;
2. 20 noded, 60 degree of freedom brick elements;
3. 13 noded, 49 degree of freedom transition elements;
4. 16 noded, 54 degree of freedom transition elements;
5. 2 noded, 12 degree of freedom beam elements.

The shell element is an eight noded curved quadrilateral thick shell element, degenerated from the 20 noded solid element (Ahmad, et al. 1970 and Puthli, 1981). Each node has five degrees of freedom, of which three are translational and two out-of-plane rotational degrees, giving a total of 40 degrees of freedom per element (see Fig. 5). Fig. 5 also shows positions and numbering of integration points related to the element coordinates and node numbering order, where the results of analyses are output. The program allows a higher number of integration points, particularly in the thickness direction, but for the present work, a total of 12 integration points will suffice in most cases. This gives a 2×2 Gauss integration along the planes of the shell, with ξ and $\eta = \pm 1/\sqrt{3}$

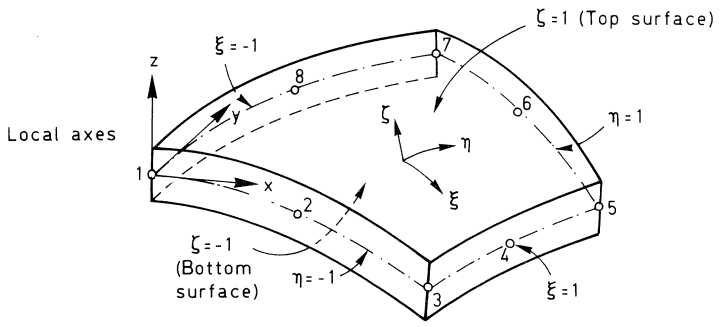

Typical element coordinate details

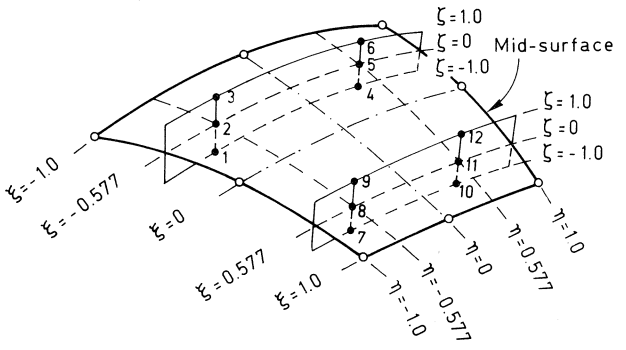

Position and numbering of integration points

Fig. 5. Thick shell element.

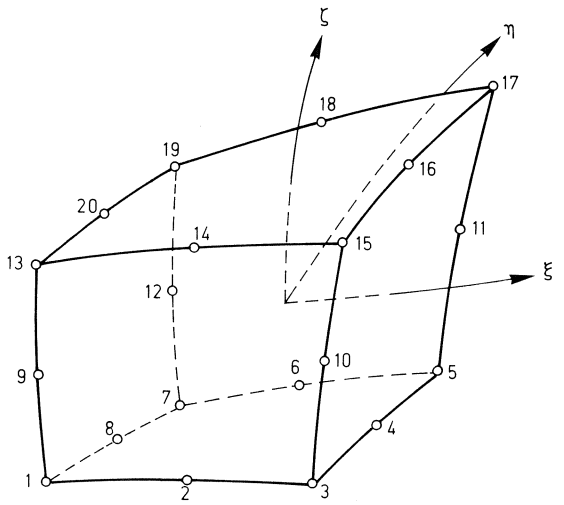

Fig. 6. Solid element.

(≈ 0.577) and 3 point Simpson integration in the thickness direction, with the three points corresponding to the bottom surface, mid-surface and top surface of the shell ($\zeta = -1.0$, 0.0 and $+1.0$) respectively.

The brick element used is the 20 noded solid isoparametric element shown in Fig. 6. An isoparametric element is described as an element having the same interpolation function for displacements and geometry (shape). A second order polynomial in ζ, η and ζ is used for this element. In general, a choice of Gauss integration order that may be used is $3 \times 3 \times 3$, $2 \times 2 \times 3$, $3 \times 3 \times 2$ and $2 \times 2 \times 2$. The minimum order of integration is $2 \times 2 \times 2$. The integration order chosen for the present work is $2 \times 2 \times 3$ in most cases. However, where brick elements are stacked together, $2 \times 2 \times 2$ order is also chosen. The order of numbering the integration points follows the sequence followed in the shell element (Fig. 5). Unlike shell elements, solid elements represent three dimensional measurements and do not explicitly imply any thickness. Therefore, Simpson integration is not provided in DIANA as an option for such elements and the positions of the integration points from the middle of the solid in each of the directions ξ, η and ζ are given for $3 \times 3 \times 3$ integration as $-\sqrt{0.6}$, 0.0 and $+\sqrt{0.6}$ (≈ 0.774). For $2 \times 2 \times 2$ integration, the positions for ξ, η and ζ are $-1/\sqrt{3}$ and $+1/\sqrt{3}$ only. The $3 \times 3 \times 3$ Gauss integration, with 27 integration points, requires a lot more computer storage and is only sparingly used. It has been found useful to model the weldment area with solid elements, as will be discussed in later chapters.

In order to combine the use of shell and brick element in the same analysis, it is useful to have "transition" elements for compatibility at the junction between the shell and solid configurations. In the present study, two types of transition elements are used. The 13 noded transition element (see Fig. 7) has only one side attached to a solid element, the opposite side to shell elements and the remaining two (adjacent) sides

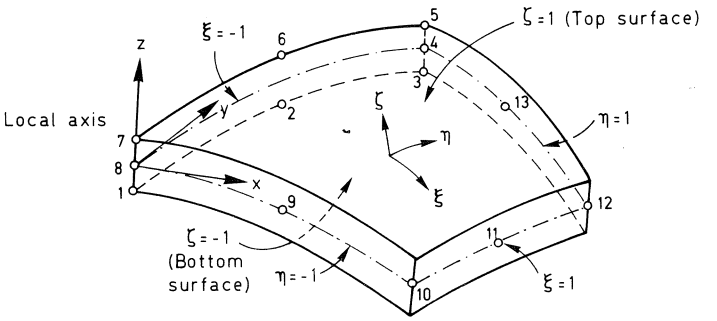

Typical element coordinate details

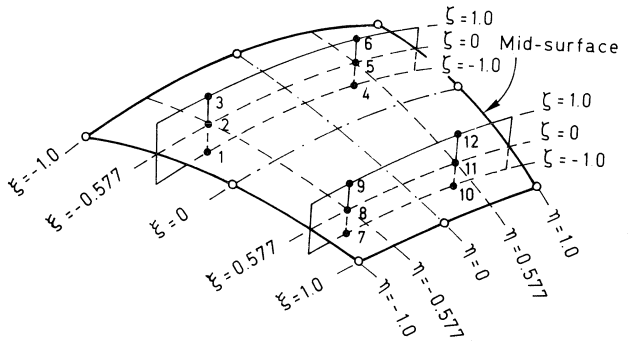

Position and numbering of integration points

Fig. 7. Transition element.

to other transition elements. The 16 noded transition element (not shown here, but similar to the 13 noded element) has two sides attached to solid elements and two sides attached to other transition elements. Details of the integration points, etc., are similar to those for the shell elements described earlier.

The beam element used for the present work is a linear beam element with two nodes. This element is only used in the present work to distribute the applied loads at the ends of members over the total cross-section. They are therefore only fictitious elements with properties given such as to induce uniform nominal stresses or strains in the members.

6 Preliminary study to establish basis for numerical modelling

The absence of reliable information on numerical modelling for strain concentration problems of joints in rectangular hollow sections is the primary reason for this initial work. X joints are one of the simpler types of joint with respect to geometry and loading,

and therefore it seems logical to study and compare analytical results with measurements on two X joint specimens with the brace loaded in tension. Experience in modelling rectangular hollow sections and weldments in joints and interpretation of the results in determining strain concentration factors has thus been gained. It must however be borne in mind that for major differences in geometry (different β ratios, etc.), it is still advisable to check the modelling. Also, checks and modifications may also be necessary for other types of joints.

Two models to be tested for the research programme (see Figs. 8 and 9) were selected and their dimensions, thicknesses, corner radii and weld details measured at a number of selected points. From geometrically symmetrical points, averaged values of the measurements were taken for use in the analysis, so that the corresponding analyses would be based on average measurements of the test specimen. The two models were both of similar geometrical properties, except that one model was roughly twice the size of the other. The main difference is that the smaller model has fillet welds, while the larger model is butt welded.

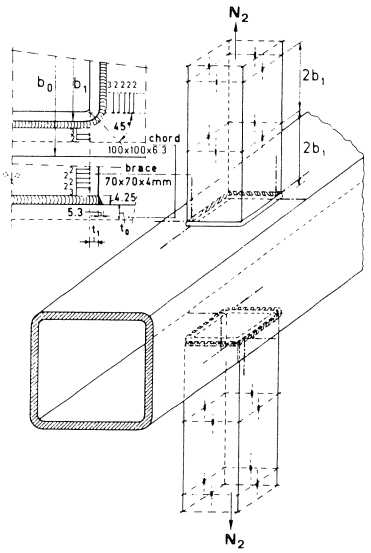

Fig. 8.
Fillet welded test specimen X1,
showing locations of strain gauges.

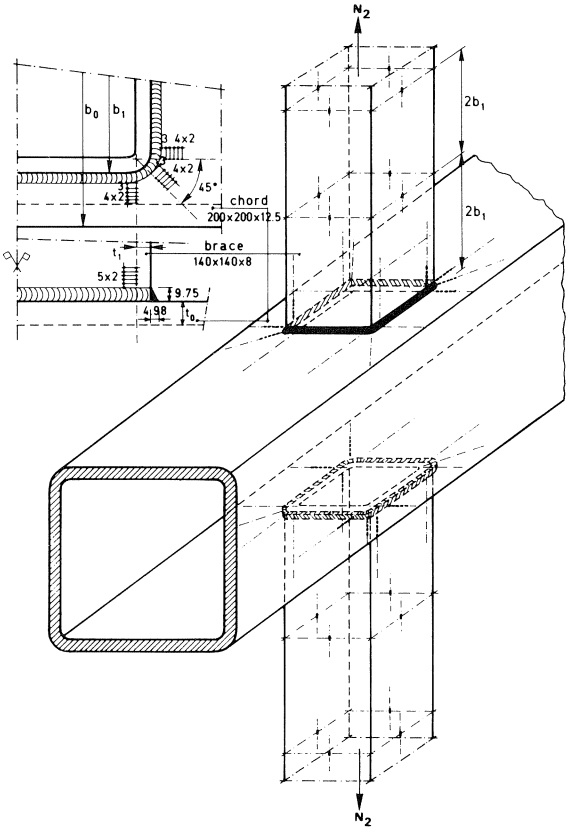

Fig. 9.
Butt welded test specimen X5,
showing locations of strain gauges.

Table 1. Chord and brace models for analysis (test specimen X-1)

Case	Chord	Braces	Comments:
1	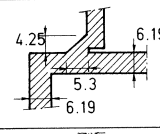	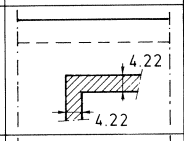	Coarse mesh
2	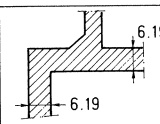	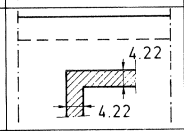	Coarse mesh. Full penetration of weld assumed
3	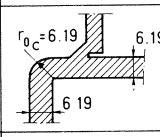	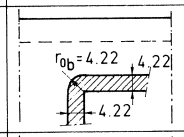	Coarse mesh
4	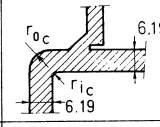	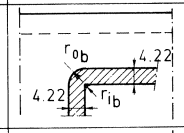	Fine mesh in cross section r_{o_c} =6.7, r_{i_c} =0.51 t_o =6.7 - 0.51 = 6.19 r_{o_b} =4.7, r_{i_b} =0.48 t_1 =4.7 - 0.48 = 4,22
5	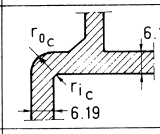	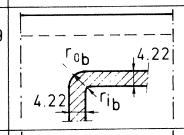	Fine mesh in cross section as in 4, but with full weld penetration
6	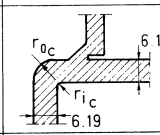	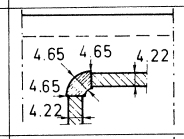	Fine mesh in cross section as in 4, but brace corner thicker
7	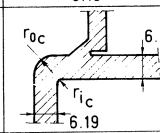	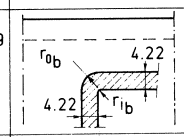	As in 4, but fine mesh in cross section and longitudinally on brace near the weld.
8	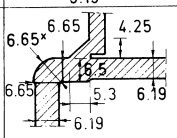	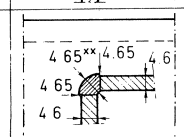	Fine mesh as for 7 x) t_o in corner cannot be more than 6.7, chosen: t_o = 6.65 xx) t_1 in corner cannot be more than 4.7. chosen: t_1 = 4.65

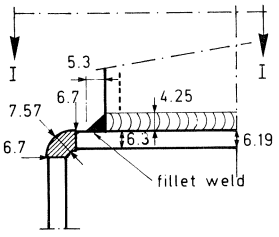

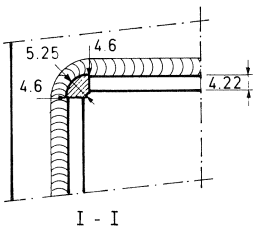

I - I

Average measurements on test specimen X-1

In order to carry out a large number of analyses for a parametric study on each type of joint, because no automatic mesh generation programs were available at the start of the programme for rectangular hollow section joints, it is essential to use simple rectangular meshes where possible. A combination of uncomplicated special purpose programs and special input generators such as PATRAN (Brebbia, 1982) can be used to quickly and simply generate the finite element meshes required. In addition, rectangular meshes are likely to give more accurate results, particularly of strains and stresses. The cross-sections of the hollow sections, particularly near and at the corners, and the weldment have been modelled in different ways as summarized in Tables 1 and 2. Two basic mesh gradations were used for these models. The coarse mesh had 6 shell elements in the brace cross-section and 9 in the chord cross-section. For the fine mesh, there were 8 in the brace cross-section and 11 in the chord cross-section. The cases with

Table 2. Chord and brace models for analysis (test specimen X-5)

Case	Chord	Braces	Comments:
9	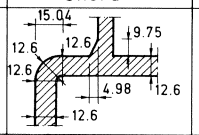	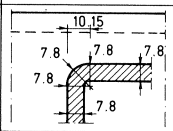	Fine mesh as for case 7 (X-1)
10	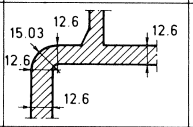	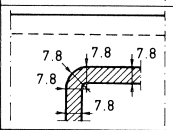	Fine mesh, more elements on chord face. comparable with case 7 (X-1)
11	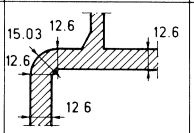	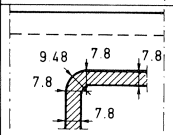	Fine mesh, more elements on chord face
12	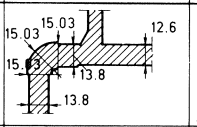	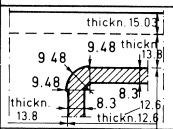	Fine mesh, more elements on chord face. (12.6 mm thickness on chord face only within closure formed by weld toe).
13	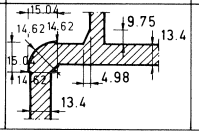	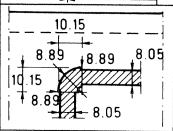	Fine mesh, more elements on chord face. $t_0 = \frac{14.2 + 12.6}{2} = 13.4$ $t_1 = \frac{8.3 + 7.8}{2} = 8.05$

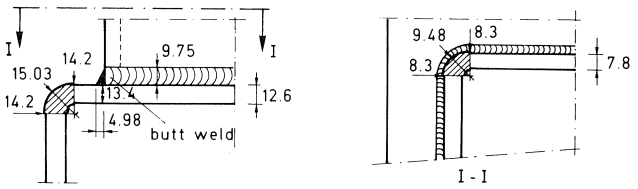

Average measurements on test specimen X-5

"fine mesh, more elements on chord face" (Table 2) indicate cases where more elements were used between the weld toe and the chord corner to trace the non-linear path of the strain gradient more accurately (see Fig. 10). Therefore, the chord cross-section for X joints with brace to chord width ratio (β) of 0.7 is invariably provided with more than 11 elements, mainly concentrated in the region of the chord face between the weld toe and the chord corner.

At the junction between the brace and chord, the fillet as well as butt welds have been modelled as brick elements. Also, the attachment of the weld to the brace and chord, as well as the region of the chord face enclosed by the brace, have been modelled with brick elements. This can be seen in the more detailed Fig. 11, which shows the modelling in the region of interest as well as the principal strains. This idealization is useful in correctly representing the attachment of members and stiffness of the material at the junction. Also, physical interpretation of the results is straight-forward. However, it is not strictly necessary to model the entire enclosed region of the chord face. It has been done here only for convenience in rapid modelling and data input.

The following general conclusions are made from this preliminary work:

- A large number of analyses using the present type of idealization (Figs. 10 and 11), is possible on a mini-computer such as a VAX 11/780 or Gould/SEL PN 9005, for X joints. For T joints, a quarter of the joint needs to be modelled, but the additional work and computer power required is only marginally more.
- It is necessary to model the brace and chord corner curvatures for a good representation, since these curvatures are relatively large. Also, the modelling of the weld and attached members in brick elements facilitates a correct representation of the stiffness and behaviour, in addition to providing a straight-forward interpretation of the output.

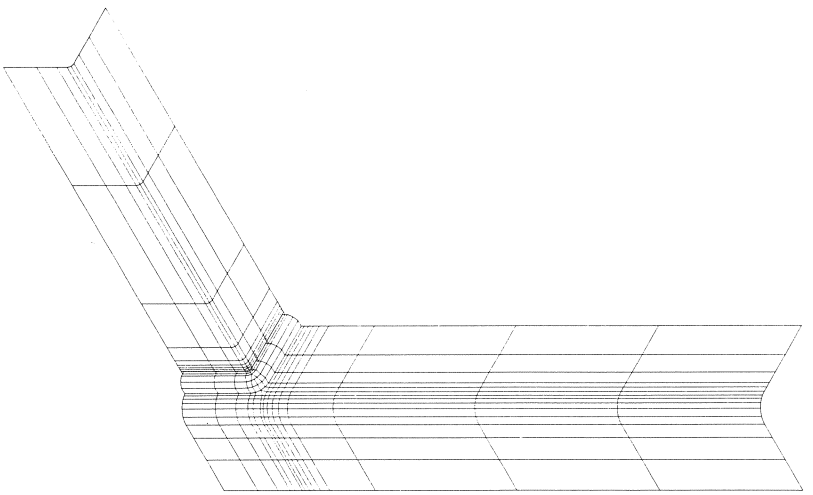

Fig. 10. Complete FE model of 1/8th X joint for braces loaded in axial tension.

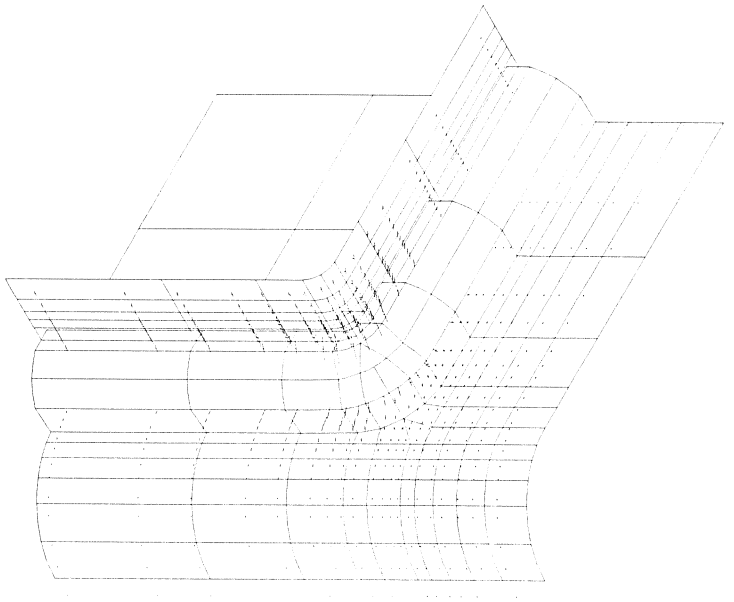

Fig. 11. Details of FE modelling of 1/8th X joint near weldment for $\beta = 0.7$, showing principal strains for braces loaded in axial tension.

- At positions remote from the high strain concentrations, the length to width ratio of some of the shell elements become unavoidably large due to the simple rectangular mesh pattern chosen for rapid data generation. Although the strains from the analyses at these positions are unlikely to be accurate, the modelling of their stiffness is adequate for determining strains in the region of high strains. In this region of interest, the length to width ratios of the shell-elements and the length/width/height ratios of the brick elements are acceptable (see Figs. 10 and 11).
- Particularly because of the simple modelling methods used, it has been found useful to calibrate the numerical model with measurements on test specimens of representative joints. This is therefore done whenever there is a change in: the type of joint (e.g.: X, T, K with gap and K with different percentages of overlap); the type of load; and any major geometrical variation such as the brace to chord width ratio (β).
- For close correlation with experimental measurements, it is necessary to model the variation of thickness in the cross-section of the chord and brace as realistically as possible.
- The modelling of the finite element mesh, together with input of the measured variations of thickness in the cross-section of the brace and chord, results in a good simulation of the strains and their gradients. Fig. 12 shows the comparisons between measurements and analysed strains for the locations in the brace and chord where the highest strains occur. The results are for case 8 (Table 1) for joint X1 and case 12 (Table 2) for joint X5.

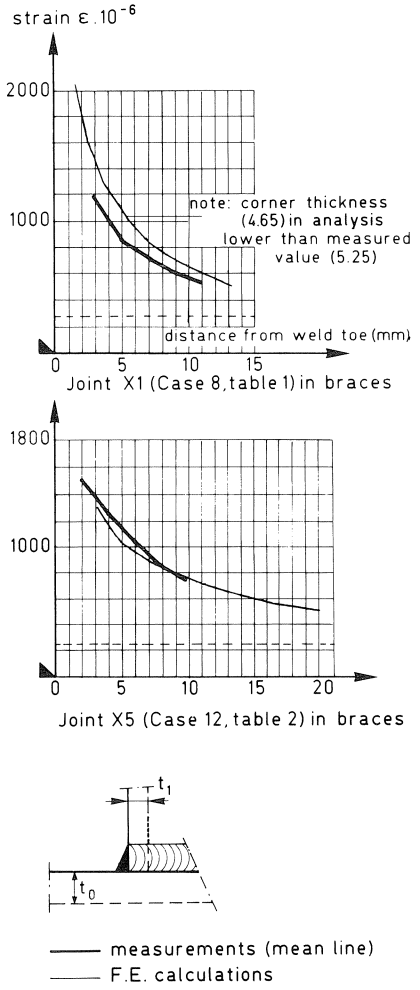

Fig. 12a.
Comparison of the strain distribution in the braces, between measurements and FE analyses.

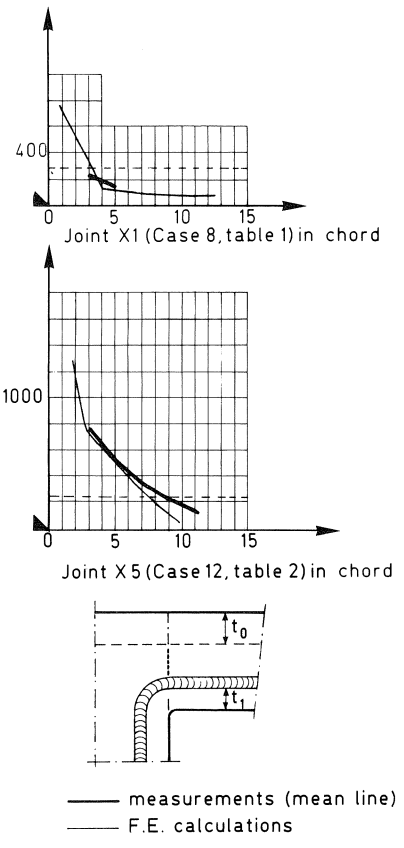

Fig. 12b.
Comparison of the strain distribution in the chord, between measurements and FE analyses.

- Because of the strong influence of the weld shape on strains close to the weld toes, measurements and finite element results in this region will be ignored in determining strain concentration factors (SNCF). The analytical or measured data will be extrapolated from outside the region, but close enough to fall inside the zone of the strain gradient caused by the global geometrical effects.
- In reality, the wall thicknesses at and near the corners of the hollow sections used in the experimental work are all higher than in the middle of the section. For the parameters where measurements are available from test specimens, two analyses have been

done. In addition to the analyses using measured dimensions as input, analyses are also carried out with nominal (specified) dimensions. Observations show a wide variation in the strains using the nominal thickness near and at the brace and chord corners. Analyses with nominal values mostly give higher strains, because the nominal thicknesses are smaller than measured thicknesses.

More detailed information on this preliminary study is given in the report by Puthli et al. (1986).

7 General procedure for determining SNCF values for parametric study

The procedure consists of four distinct steps. The first is the experimental testing of some representative joints, where at low load levels, strains and strain gradients are measured in the linear range prior to fatigue testing. Secondly, two numerical analyses are carried out for comparison with the experiments, where the first model has dimensions based on average dimensional measurements of the test specimen, as discussed in chapter 6, while the second model uses nominal (specified) dimensions. Thirdly, a number of joints with parametric variations (of β, 2γ and τ) are analysed using nominal dimensions, which also include the representative joints in the set. This last analytical work forms the basis for determining parametric formulae, which, together with an analysis of all previous work, is the last (fourth) step of the procedure.

For rectangular hollow section joints where, dependent upon the type of joint, the geometric stress (or strain) gradient can be strongly non-linear, no information is available for hot spot strain definition. A hot spot strain definition based upon linear extrapolation was accepted in Working Group III of the ECSC Offshore Programme for joints in circular hollow sections. It was determined later that even in circular hollow section joints, strain distribution is non-linear for particular joints. Consequently, the IIW recommendations (1985) no longer specify any method of extrapolation. Therefore, two methods of extrapolation of experimental and numerical results to the weld toe are applied in order to determine geometric hot spot strain and strain concentration factors (SNCF), namely, a linear extrapolation and a quadratic extrapolation from within limits are given in Fig. 13. The region of influence of notch strain to be ignored is taken as $0.4t$ (for $t \geq 10$ mm) or 4 mm (for $t < 10$ mm), following the procedure for circular hollow sections.

For linear extrapolation, the limit of $0.6t$ for the region of linear extrapolation A to B in Fig. 13 is based upon A being $1.0t$ away from the weld toe C, when $t \geq 10$ mm. However, when $t < 10$ mm, because B in Fig. 13 is always 4 mm away from weld toe C, the data points used in the extrapolation at A and B would be too close to each other if A were stated to be $1.0t$ away from C. Therefore, by allowing length A–B to be always $0.6t$, this problem is overcome.

For quadratic extrapolation, the same philosophy for points D, E and F is applied as points A, B and C for linear extrapolation. The only difference from the linear extrapolation is that length D–E is taken slightly longer at $1.0t$ instead of $0.6t$, in order to be

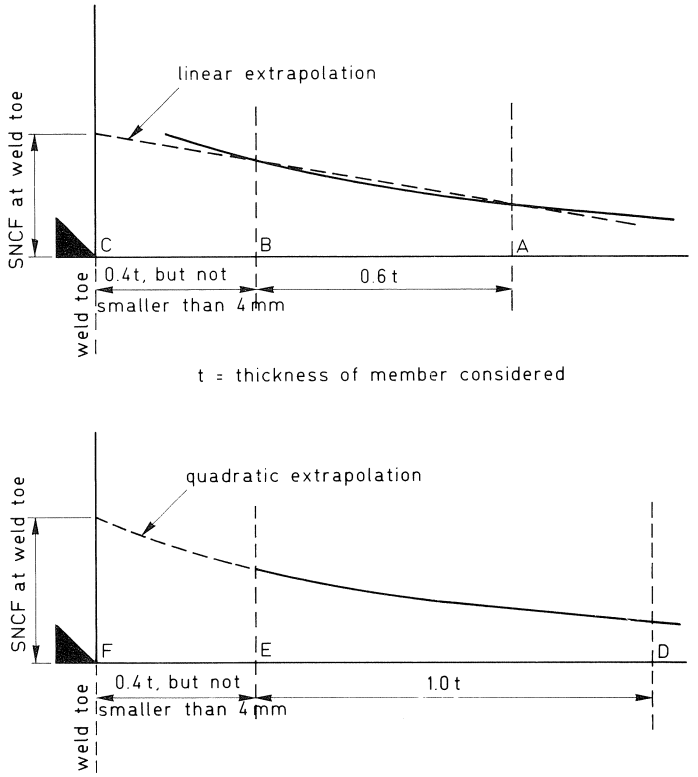

Fig. 13. Methods of extrapolation.

able to take sufficient data points between D and E for greater accuracy in the quadratic extrapolation to the weld toe F.

For joints in rectangular hollow sections, where the geometric strain can be strongly non-linear, quadratic extrapolation gives more realistic values for the SNCF, which is supported by the test results.

All results are presented by normalizing strains in the brace as well as chord with respect to nominal longitudinal strain ($\varepsilon = 1.0$) in the brace. This applies to experimental and numerical work, allowing direct comparisons, so that extrapolated values directly give SNCF values.

7.1 *Procedure for experimental work*

The primary reason for experimentation is to determine fatigue data for the joints from constant amplitude fatigue testing at two different stress ranges (S_r), so that $S_{r\,h.s.}$-N_f (or $\varepsilon_{r\,h.s.}$-N_f) lines similar to those in Fig. 2 may be obtained for square hollow section joints. Fatigue failure (N_f) is deemed to have occurred in the brace when a through thickness crack in the brace extends over the complete width of any one side of the brace. Fatigue failure (N_f) in the chord is deemed to have occurred when a through

thickness crack in the chord extends over a length equal to the brace width plus the weld projections on the chord at both ends. This deviates somewhat from the criterion used for circular hollow sections (IIW, 1985). However, the deviation in fatigue life is not so large. The size (or thickness) effect is measured primarily on the X joints, where for one representative joint having average parameters in the whole parametric range, 3 different joint sizes with almost identical parameters are tested (chord width = 100, 200 and 260 mm). The stress ratio (R) which is generally chosen for all tests is $R = +0.1$. However, $R = +0.5$ is also used, but this time on T joints, in order to determine the influence of R. Prior to the fatigue testing of all joints, strains are measured at preselected measurement lines where peak strains are known to occur. Strain gauge chains are placed at these locations to fall sufficiently within and outside the extrapolation limits.
At least 4 test specimens with the same geometry and dimensions are used for the fatigue tests, a pair at two different stress ranges (S_r). Measurements of strain and determination of SNCF are also carried out for all these specimens. As expected, a scatter exists in the strain distribution along the measurement lines at identical locations. In general, this scatter is influenced by small differences in wall thickness, corner radii and weld dimensions. Where possible, the SNCF values (experimental measurements) are recorded for 3 cases if the fatigue testing is also carried out. These are at locations where the first crack occurs during fatigue testing ($SNCF_{crack\ loc.}$), where the maximum SNCF distribution occurs ($SNCF_{max}$) and for the average SNCF distribution ($SNCF_{average}$).

7.2 *Procedure for comparison of experiments with numerical modelling*

A comparison is carried out between experiments and two numerical analyses for each joint that is tested with one set of non-dimensional parameters. The first analysis for each such joint is based upon the average measured dimensions for one selected joint out of a series in the fatigue tests with the same parameters, the strain measurements of which are used for the comparison. The second analysis uses nominal (specified) dimensions.
This work is carried out for two primary reasons. First, with the analysis using measured dimensions, to check the accuracy of the numerical modelling against experimental measurements. Secondly, to observe how far the strains and SNCF values for analyses with nominal dimensions deviate from the SNCF values obtained from experimental measurements, and provide useful background data on margins of safety with respect to actual joints made of hot finished hollow sections.

7.3 *Procedure for numerical analyses of strains and tabulation of strain concentration factors (SNCF) using nominal dimensions*

This work forms the bulk of the analytical work. Limits of variation of the non-dimensional parameters β, 2γ and τ are set and a number of values chosen including those representative ones already tested. The same scale is used for all the analyses, with the chord widths invariably kept constant and the specified nominal dimensions used. Butt

Table 3a. Butt welded X joints analysed (nominal dimensions)

$\beta =$	$2\gamma = b_0/t_0 = 25$			$2\gamma = b_0/t_0 = 16$			$2\gamma = b_0/t_0 = 12.5$		
b_1/b_0	chord	braces	no.	chord	braces	no.	chord	braces	no.
0.25				200 × 200 × 12.5	50 × 50 × 6.3	XC-42			
				200 × 200 × 12.5	50 × 50 × 12.5	XC-43			
0.4	200 × 200 × 8	80 × 80 × 4	XC-20	200 × 200 × 12.5	80 × 80 × 4	XC-21	200 × 200 × 16	80 × 80 × 4	XC-22
	200 × 200 × 8	80 × 80 × 8	XC-23	200 × 200 × 12.5	80 × 80 × 8	XC-24	200 × 200 × 16	80 × 80 × 8	XC-25
0.55				200 × 200 × 12.5	110 × 110 × 6.3	XC-44			
				200 × 200 × 12.5	110 × 110 × 12.5	XC-45			
0.7	200 × 200 × 8	140 × 140 × 5	XC-26	200 × 200 × 12.5	140 × 140 × 5	XC-27	200 × 200 × 16	140 × 140 × 5	XC-28
	200 × 200 × 8	140 × 140 × 8	XC-29	200 × 200 × 12.5	140 × 140 × 8	XC- 5	200 × 200 × 16	140 × 140 × 8	XC-30
				200 × 200 × 12.5	140 × 140 × 12.5	XC-31	200 × 200 × 16	140 × 140 × 12.5	XC-32
				100 × 100 × 6.3	70 × 70 × 4	XC- 1			
				260 × 260 × 16	180 × 180 × 10	XC- 9			
0.85				200 × 200 × 12.5	170 × 170 × 6.3	XC-46			
				200 × 200 × 12.5	170 × 170 × 12.5	XC-47			
1.0	200 × 200 × 8	200 × 200 × 6.3	XC-33	200 × 200 × 12.5	200 × 200 × 6.3	XC-34	200 × 200 × 16	200 × 200 × 6.3	XC-35
	200 × 200 × 8	200 × 200 × 8	XC-36	200 × 200 × 12.5	200 × 200 × 8	XC-37	200 × 200 × 16	200 × 200 × 8	XC-38
				200 × 200 × 12.5	200 × 200 × 12.5	XC-39	200 × 200 × 16	200 × 200 × 12.5	XC-40
							200 × 200 × 16	200 × 200 × 16	XC-41

—— also test specimen (fillet welded if brace wall thickness $t_1 < 8$ mm)
---- also analysed as fillet welded joints

welds are modelled for all joints. However, some extra joints are also analysed with fillet welds, so that the influence of weld type can be studied.
All the strain concentration factors for nominal dimensions as well as for representative experimentally determined values are tabulated elsewhere (De Koning, et al. 1988) for further processing into fatigue design recommendations. These are done for both linear and quadratic extrapolation methods.

7.4 *Procedure for making design recommendations*

The fatigue design recommendations involve provision of $S_r - N_f$ or $\varepsilon_r - N_f$ lines and parametric formulae for SCF or SNCF. The present work will concentrate on provision of SNCF formulae and graphs. Where possible, factors will be given to account for weld type, variation in actual measurements of hot finished hollow sections from nominal values and conversion from SNCF into SCF for the convenience of designers.

8 Study on X joints with axial tension in braces

Table 3 gives the parametric variations chosen for the study (De Koning, et al. 1988; Puthli, et al. 1988), together with the nominal dimension used. Butt welds are more likely to be present and the study is therefore primarily on the basis of butt welded joints. Some additional work is also done on fillet welded joints as indicated in Table 3a, in order to include the effect of weld type on the geometric strain concentration factors. Details of weld dimensions used in the analyses with nominal dimensions is given in Fig. 14.
The joints chosen to be made into test specimens are indicated in Table 3a. The three test specimens for $\beta = 0.7$, $2\gamma = 16$ (XC1, XC5 and XC9) are identical joints, each of a

Table 3b. Nominal corner radii of outer surface of hollow sections

square hollow section	used as:	nominal outer surface corner radius (r_0)
70 × 70 × 4	bracing	4.5*
80 × 80 × 4	bracing	4.5*
80 × 80 × 8	bracing	8.5*
100 × 100 × 6.3	chord	6.8*
140 × 140 × 5	bracing	7.0
140 × 140 × 8	bracing	11.2
140 × 140 × 12.5	bracing	17.5
180 × 180 × 10	bracing	20.0
200 × 200 × 6.3	bracing	12.6
200 × 200 × 8	chord and bracing	16.0
200 × 200 × 12.5	chord and bracing	25.0
200 × 200 × 16	chord and bracing	32.0
260 × 260 × 16	chord	32.0

* this radius is assumed to be 0.5 mm larger than specified in the hollow section tables, in order to model the corner elements as cylindrical shell elements

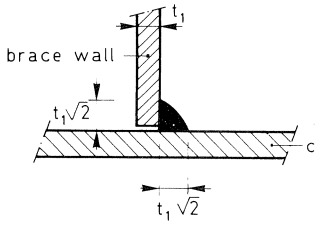

Fig.14a. Fillet weld, when $t_1 < 8$ mm.

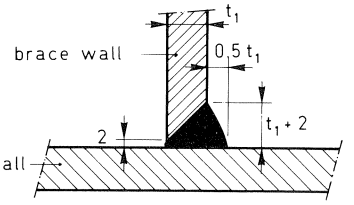

Fig. 14b. Butt weld, when $t_1 \geqq 8$ mm.

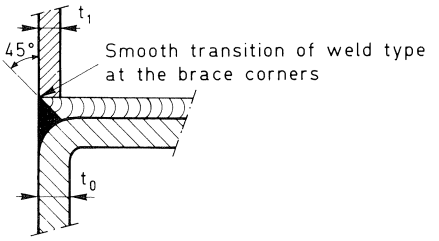

Fig. 14c. Weld detail for joints with $\beta = 1.0$.

Fig. 14. Weld details used for analyses with nominal dimensions.

different size (chord widths 100, 200 and 260 mm respectively), and chosen primarily for including the size (thickness) effect into the fatigue data. The two test specimens with $\beta/2\gamma$ values of 0.4/25 and 1.0/12.5 are included for control of the numerical work over a range of parameters in β and 2γ.

Hot finished hollow sections with steel grade Fe 430 D and Fe 430 B, in accordance with Euronorm 25–72, are used for the specimens. All test specimens are welded with rutile electrodes (trade name OMNIA) in accordance with NEN 1062 (ERa 112), NBN F 31-001 (E43-2R), ASME SFA-5.1 (E6013), DIN 1913 (E43 22R(C)3), ISO 2560 (E432R12)

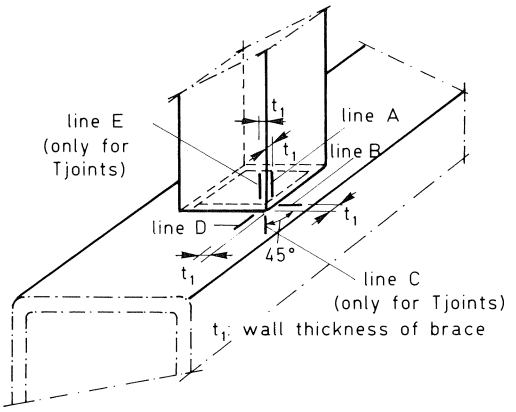

Fig. 15a. Lines considered for SNCF (for $\beta = 0.4$ and 0.7).

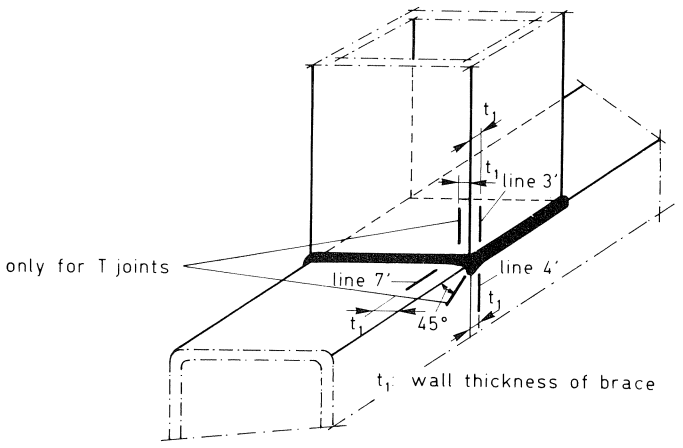

Fig. 15b. Lines considered for SNCF (for $\beta = 1.0$).

and BS 639 (E43 22R). Fillet welds are provided at the joints for all brace wall thicknesses below 8 mm and butt welds for 8 mm and above. The fillet welds are carried out in 3 runs and the butt welds in 4 runs.

Fig. 15 shows lines that are considered for determining geometrical SNCF values at weld toes, where both linear and quadratic extrapolation methods are considered. Figs. 16 and 17 show the complexity of modelling the elements at the joint for $\beta = 1.0$. The PATRAN system (see Brebbia, 1982) has been used to model all joints with $\beta = 1.0$

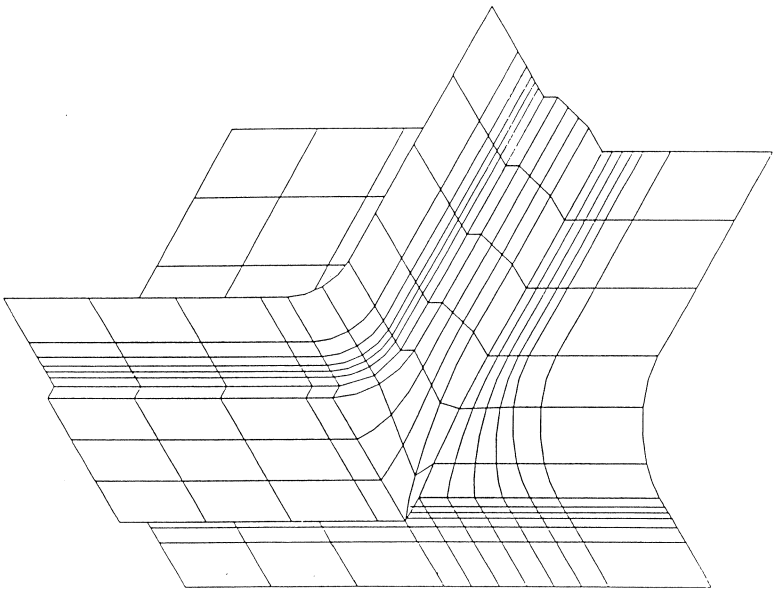

Fig. 16. Details of FE modelling of 1/8th X joint near weldment, for $\beta = 1.0$ (view from outside of joint).

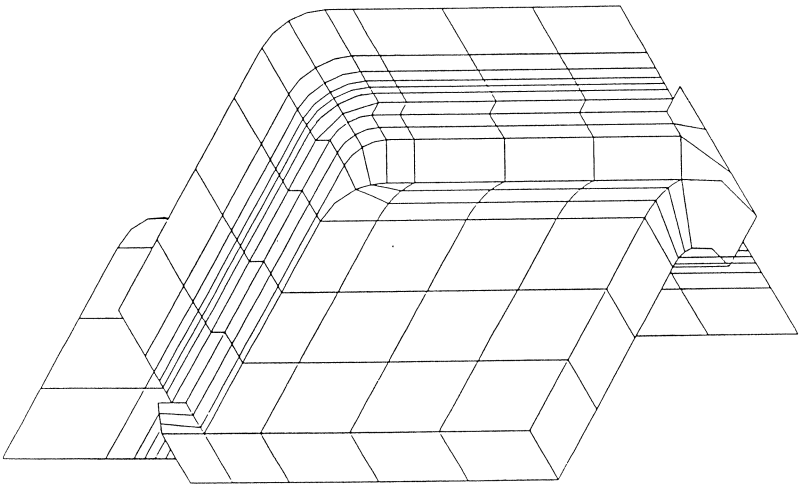

Fig. 17. Details of FE modelling of 1/8th X joint near weldment, for $\beta = 1.0$ (view from inside of joint).

because of the complexity of the joint details. For $\beta = 0.4$ and 0.7, special purpose mesh generators have been written to develop the models. Fig. 18 shows photographs of the strain gauged X joint specimen with $\beta = 1.0$, indicating the complexity of the welding details in transition from a fillet weld to a butt weld at the (critical) corners.
Fig. 19 shows a typical comparison between the experimental measurements of strain and the two analyses using measured dimensions of the test specimen and the nominal (specified) dimensions. This comparison is for the line B in the chord for XC5 ($\beta = 0.7$, $2\gamma = 16$), where the chord width is 200 mm. Fig. 19 illustrates the distinct variation of the strains for the analysis with nominal dimensions from the experimental strain measurement as well as the analysis using measured dimensions of the test specimen. The values for joints with nominal dimensions are invariably higher, because the nominal dimensions in the corners are smaller than actual dimensions, giving higher strains (or stresses) on the outer surfaces for the same applied forces. It is also noted that thicknesses taper from the corners towards the middle of the sides and that measured corner radii of the square hollow section specimens are smaller than nominal values. Also, the variation between nominal and measured values appears to be larger for smaller joints, which is reflected in the strain measurements. However, the strain distribution from the analyses with use of measured dimensions have a good correlation with the test measurements, giving confidence in the modelling approach.
Using the finite element modelling approach discussed so far, numerical (FE) analyses have been carried out on all 31 joints given in Table 3a. Using the linear and quadratic extrapolation methods described so far, the SNCF values have also been tabulated (see De Koning, et al. 1988). It may be noted that for $2\gamma = 16$, more β values have been investigated, so as to investigate the influence of β more closely, within limits of $\beta = 0.25$ to 1.0.

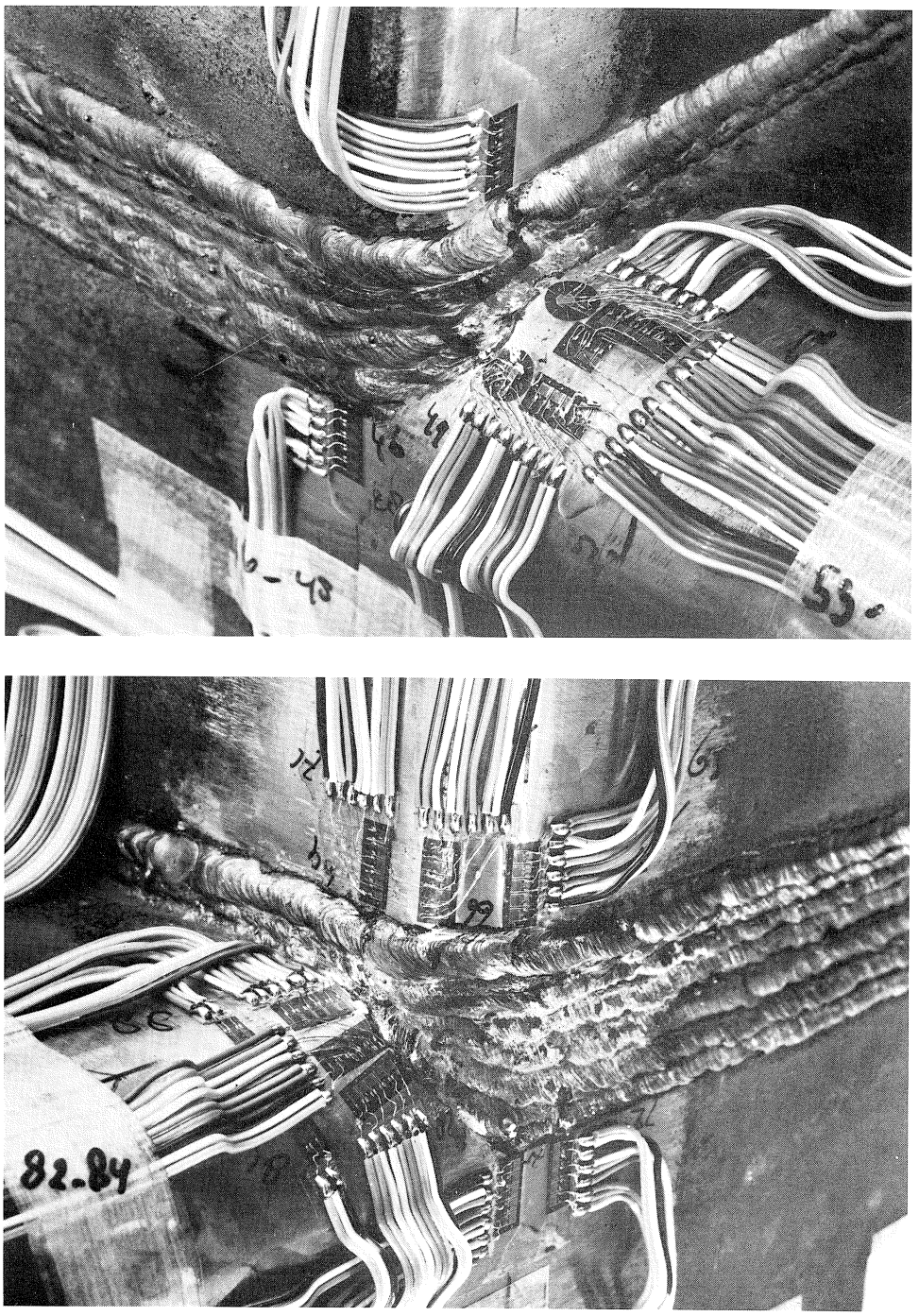

Fig. 18. Weld details at two corners between brace and chord for X joint specimen X38 with $\beta = 1.0$.

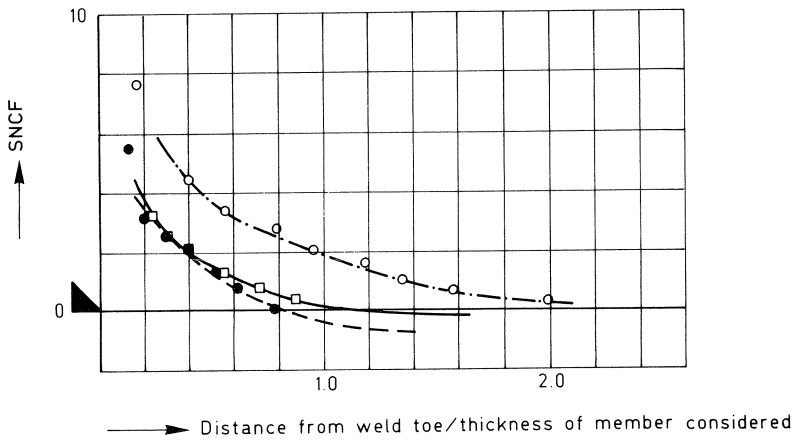

X-5 nominal dimensions
chord:
200x200x12.5mm
braces:
140x140x8.0mm

X-5 measured dimensions
chord:
200.6x200.6x12.6mm
braces:
139.8x139.8x7.8mm

F.E analysis: o
(nominal dimensions)

F.E analysis: •
(measured dimensions)

Measurements: □

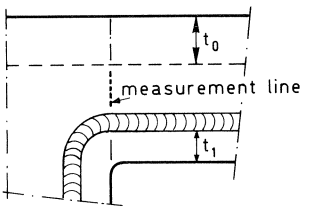

Fig. 19. Typical comparison of SNCF between test measurements and analyses.

Table 4. Interim formulae for the SNCF at the weld toe in brace and chord of butt welded X joints in RHS

method of extrapolation	location		SNCF formulae (butt welded joints), with the following limits: $\beta = 0.4$ to 1.0; $2\gamma = 12.5$ to 25.0, $\tau = 0.25$ to 1.0
	brace	chord	
linear	line A	-	$SNCF = (0.387 - 3.187\beta + 9.24\beta^2 - 5.95\beta^3)(2\gamma)^{(1.65-1.18\beta)}$
	-	line B	$SNCF = (12.53 - 41.67\beta + 48.54\beta^2 - 19.37\beta^3)\beta^2\tau(2\gamma)^{1.293}$
	-	line D	$SNCF = (21.48 - 68.68\beta + 74.41\beta^2 - 27.05\beta^3)\beta^2\tau(2\gamma)^{0.771}$
quadratic	line A	-	$SNCF = (0.447 - 3.514\beta + 9.367\beta^2 - 5.85\beta^3)(2\gamma)^{1.83-1.32\beta)}$
	-	line B	$SNCF = (12.64 - 43.13\beta + 51.55\beta^2 - 21.03\beta^3)\beta^2\tau(2\gamma)^{1.328}$
	-	line D	$SNCF = (23.65 - 75.4\ \beta + 81.55\beta^2 - 29.6\beta^3)\beta^2\tau(2\gamma)^{0.774}$

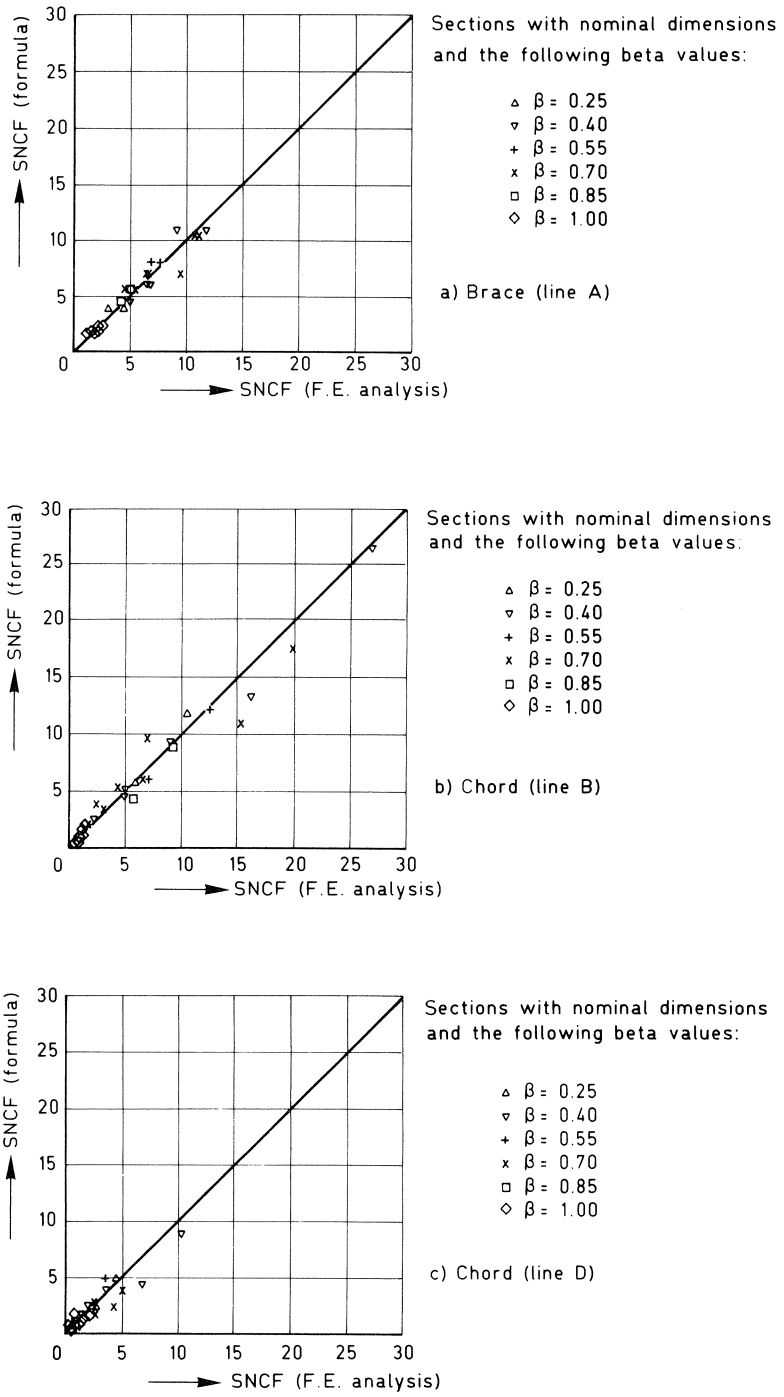

Fig. 20. Comparison of quadratically extrapolated SNCFs between FE analyses and formulae.

Table 4 gives details of the formulae obtained for the SNCF of butt welded joints using regression analysis. Fig. 20 gives a comparison between the quadratically extrapolated SNCFs from the formulae and those from the numerical analyses, for the three lines A, B and D (see Fig. 15). Similar relationships are also provided for linearly extrapolated SNCFs (see De Koning et al. 1988). The lowest correlation coefficient is 92.7%. It may be noted that the limits of β are set at 0.4 to 1.0 and not 0.25 to 1.0. This is because only 2 data points are available for $\beta = 0.25$, and although they are useful in the total regression analysis to determine the joint behaviour, could give misleading information for 2γ values other than 16. Also, β values for rectangular hollow section joints under 0.4 are uncommon.

Calculations have been carried out to determine the relationship between the SNCF values obtained from measurements on the test specimens and the FE analyses with nominal dimensions to take into account dimensional tolerances with size. This is

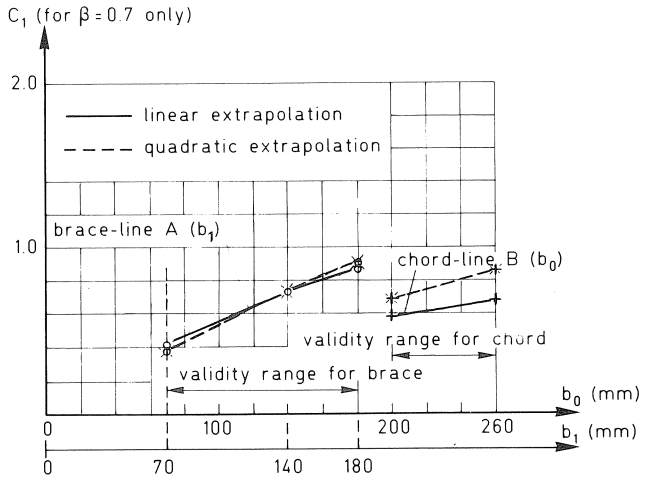

Fig. 21. Factor C_1 to account for dimensional tolerance with respect to the nominal size for the tested joints ($\beta = 0.7$ only) when determining SNCF.

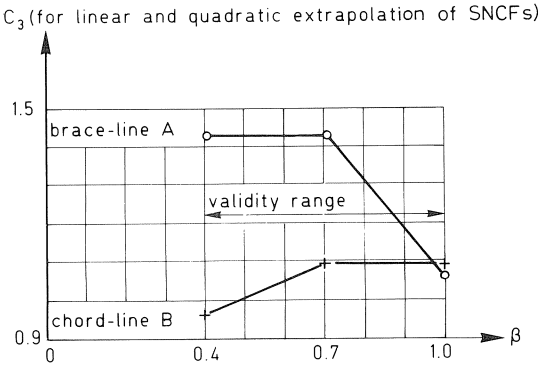

Fig. 22. Factor C_3 to account for the larger SNCF values in fillet welded specimens.

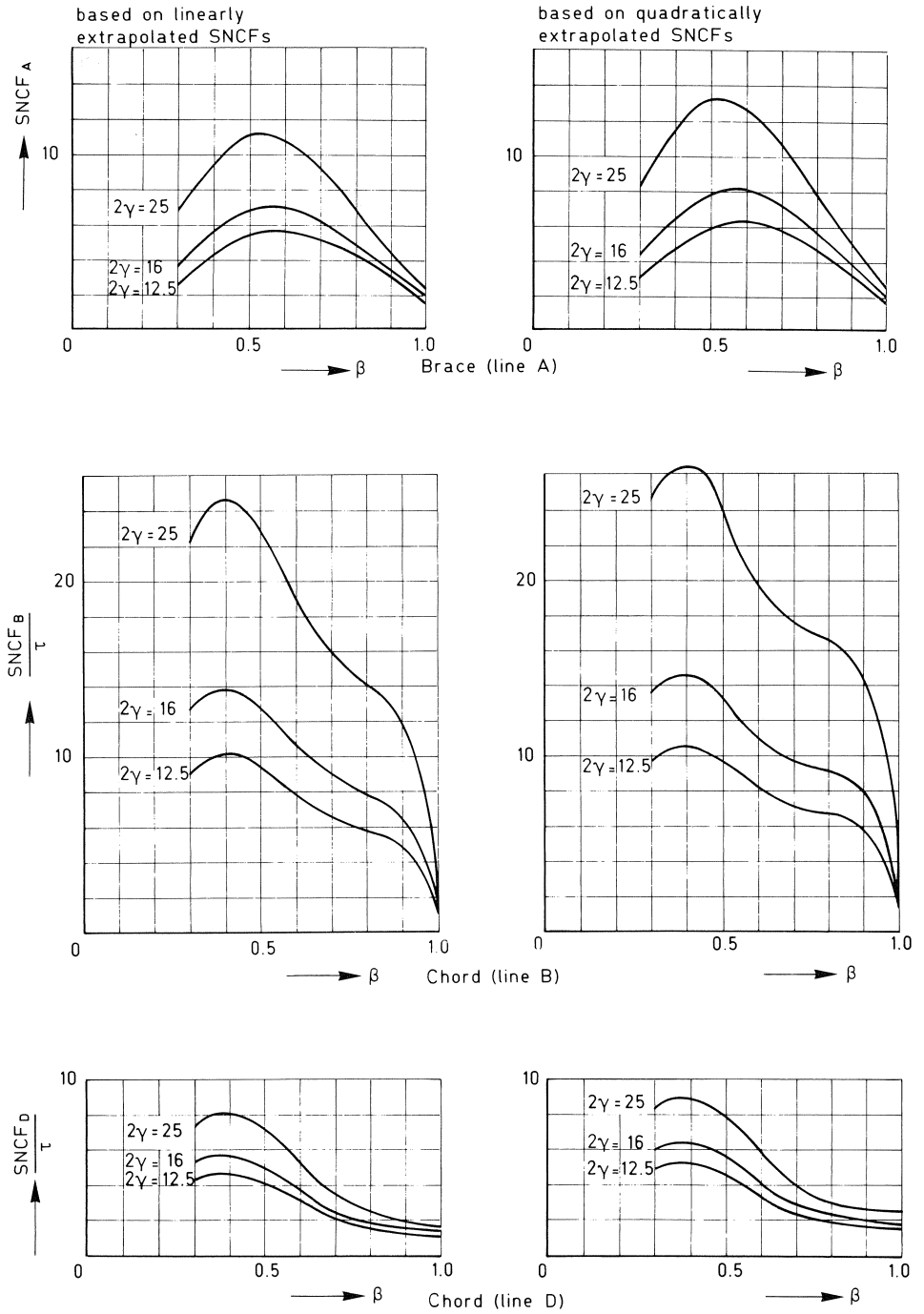

Fig. 23. Relationship between the ratio $\beta = b_1/b_0$ and the SNCF values from formulae, at the weld toe for axially loaded butt welded X joints.

given graphically in Fig. 21, as a factor C_1, for the joints that have been investigated. Similarly, for conversion of SNCF into SCF, a factor $C_2 = 1.10$ has been taken for the time being, which is based upon preliminary observations of results from experiments and numerical work. Finally, the FE work with nominal dimensions gives larger SNCF values for fillet welded joints than for butt welded joints and a conversion factor C_3 has been evaluated to multiply with the SNCF formulae in order to get SNCFs for fillet welded joints. The factor C_3 is shown graphically in Fig. 22. In addition to the complete study on butt welded joints, the few joints also analysed with fillet welds for determining C_3 are indicated in Table 3a.
Finally, the interim SNCF formulae are illustrated graphically in Fig. 23. These results can be developed further in conjunction with the work on T and K joints in order to provide firm design guidelines on a unified basis.

9 Study on T joints with axial tension or moment in the brace

The discussion on T joints (Van Wingerde et al. 1988) will be kept brief. This is partly because there is much in common with X joints on the basic experimental and analytical approach and partly because the parameters and sizes of the hollow sections are identical to those for X joints (see Table 3). Only one additional joint is considered for T joints, namely chord = 200 × 200 × 12.5 and brace = 140 × 140 × 6.3. Also, the results of the work on T joints are now in the process of being analysed, with final conclusions and suggested recommendations to be reported in the form similar to De Koning et al. (1988).
As mentioned earlier, the experimental work on T joints concentrates on two different stress ratios, $R = +0.1$ and $R = +0.5$, in order to observe the influence of R on fatigue life. As with X joints, two fatigue tests are carried out for two stress ranges for each parametric variation. Therefore, four tests are carried out for each stress ratio, giving a total of 8 tests per parametric variation. This has meant that only 2 parametric variations are chosen for the fatigue tests and also for the measurements of strain. These are for $\beta = 0.7$, $2\gamma = 16$, $\tau = 0.4$ (chord = 200 × 200 × 12.5 mm, brace = 140 × 140 × 5.0 mm) and $\beta = 0.7$, $2\gamma = 16$, $\tau = 0.64$ (chord = 200 × 200 × 12.5 mm, brace = 140 × 140 × 8.0 mm), as shown in Table 3. All tests are carried out only for axial tension in the brace. The SNCF values are determined for all work on T joints in exactly the same way as for X joints, using linear and quadratic extrapolation. All the values along the five lines A, B, C, D and E (shown in Fig. 15) are required, whereas only lines A, B and D are used for X joints.
The experimental measurements on each of the two test specimens are compared with two analyses using measured dimensions and nominal dimensions in the same way as for X joints. After obtaining a good correlation between the experimental work and numerical analyses with measured dimensions, the main analytical work on T joints, using nominal dimensions of the hollow sections, has been carried out. In keeping with the work on X joints, butt welds are modelled for all joints, with some joints also re-analysed using fillet welds.

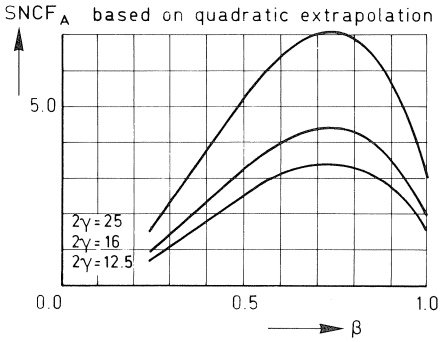

Fig. 24a. Chord (line A).

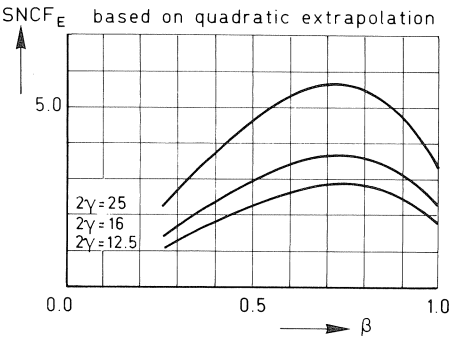

Fig. 24e. Chord (line E).

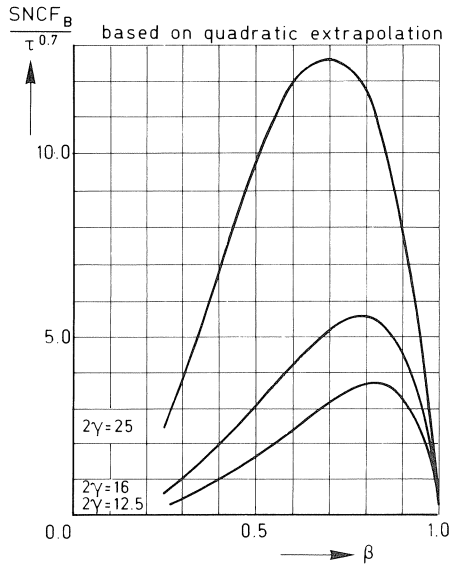

Fig. 24b. Brace (line B)

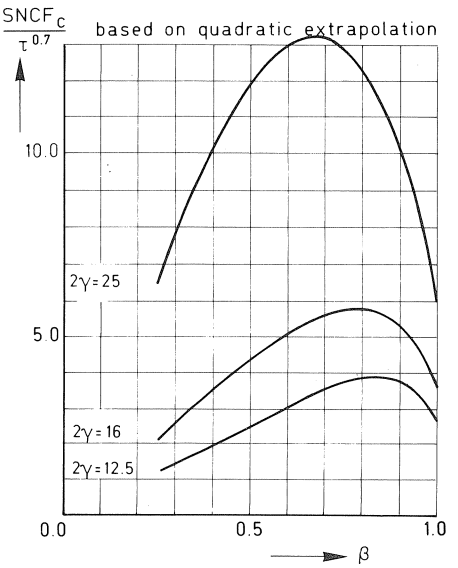

Fig. 24c. Brace (line C).

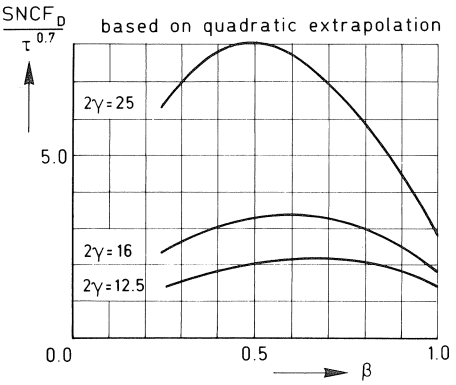

Fig. 24d. Brace (line D).

Fig. 24. SNCF formulae for butt welded T joints, with in-plane bending in the brace.

Using nominal dimensions, the cases chosen for axial loading in the brace are the joints in Table 3 with $\beta = 0.4, 0.7, 1.0$ and $2\gamma = 16$ only. For in-plane bending moment in the brace, all the same hollow section sizes and parameters as chosen for X joints in Table 3 are analysed. For $\beta = 0.4, 0.7$ and 1.0, and brace wall thickness $t_1 < 8$ mm, the numerical analyses for all joints and loading cases (axial tension in brace or bending moment in brace) are carried out with fillet welds as well as with butt welds between brace and chord. The numerical work consists of 30 FE analyses with a butt weld and in-plane moment in the brace, 9 FE analyses with a fillet weld and in-plane moment in the brace, 8 FE analyses with a butt weld and axial force in the brace, and 3 FE analyses with a fillet weld and axial force in the brace.
As with X joints, regression analyses will be carried out on the SNCFs determined and tabulated from the above analyses, to provide SNCF formulae. An interim version of the SNCF formulae for all the lines A, B, C, D and E for butt welded joints under in-plane moment are presented in Fig. 24, for quadratically extrapolated SNCF values.

10 Study on the effect of axial tension and bending in the braces of K joints with gap on the strain concentration factors

K joints are normally found in Warren type girders. As mentioned earlier in chapter 4, the investigation on fatigue strength of joints in rectangular hollow sections is being jointly carried out in Germany and the Netherlands. The work on square hollow section K joints with gap and overlap is being carried out at Universität Karlsruhe (Mang et al. 1988a, 1988b, 1988c, 1988d). However, some supplementary work, exclusively on strain concentration factors of K joints with larger dimensions (twice the size), is also being conducted at the Delft University of Technology and IBBC-TNO, Rijswijk (Van Dooren et al. 1988).
Only the work on K joints with gap, using the larger square hollow sections, is presented here, in order to illustrate the method of approach. This is because of the radical difference in the geometry, loading and behaviour of K joints with either gap or overlap, in comparison to X and T joints. Also, the intention of the work presented here is to primarily illustrate the effect that axial tension and bending have on the SNCF magnitudes of K joints with gap. Different geometrical parameters are considered and SNCFs determined at several critical locations. The K joints with gap presented here have members in square hollow sections and no eccentricity of system lines, with both braces being identical in size and the angle between braces and chord being 45 degrees (see Fig. 4), so that the gap dimension is dependent upon β. One experimental test (linear static test only), for measuring strains at critical positions is carried out, so that the SNCF values obtained from them may be used to check the FE work. The dimensions chosen are the same as for one of the joints in the FE work. Also, some initial modelling investigations and ten FE analyses using nominal dimensions are carried out.
It may be pointed out here that SNCF values for K joints with gap are generally lower than for X and T joints. Also, the strain distribution is not as strongly non-linear as for X and T joints. For dominant SNCFs, the difference between SNCFs determined by

linear and quadratic extrapolation (see chapter 7) is small. Also, in the work on X joints (De Koning et al. 1988), it is mentioned that quadratic extrapolation is proposed for the final recommendations on X joints because it gives more realistic values. Therefore, in order to have a unified approach, the work presented here on K joints with gap considers quadratic extrapolation.

10.1 *Loading and boundary conditions on K joints with gap and no eccentricity of system lines*

In spite of zero eccentricity of system lines, it can be shown that, if a girder consisting of K joints is analysed with beam elements, assuming all joints to be completely rigid, considerable bending moments can occur in addition to axial load at the joints (see Van Dooren et al. 1988). This is because of the displacements and rotations at the joints, with the magnitude of moments depending upon the location of a joint in the girder. In reality, the joints are neither hinged nor completely rigid, each joint having its own stiffness, dependent upon the joint geometry. Also, the stiffness distribution at the joint is not uniform.

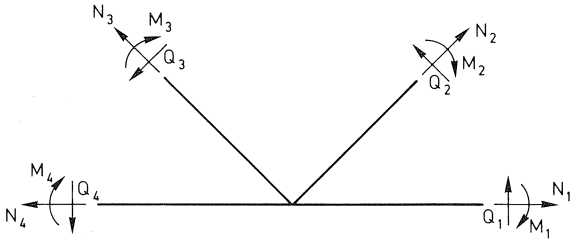

Loads acting on a K-joint

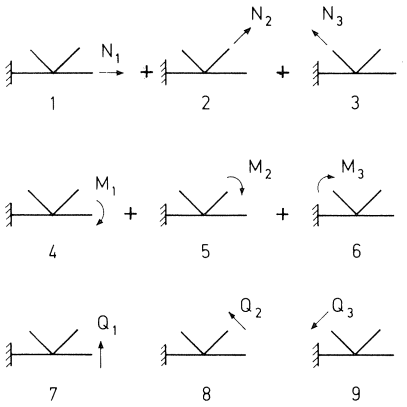

Basic load cases

Fig. 25. Isolation of basic load cases.

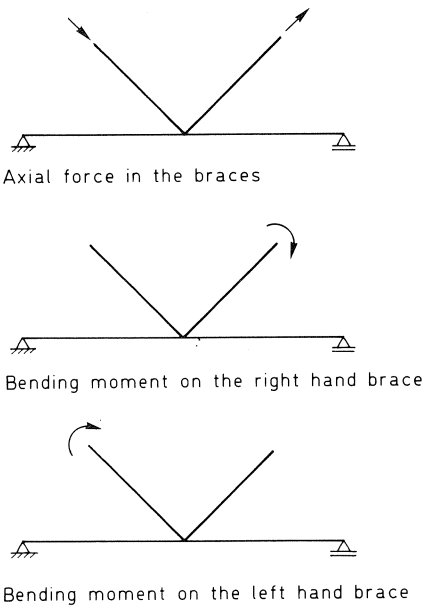

Fig. 26. Boundary conditions and load combinations used for the FE analyses on K joints.

The loading on a K joint is therefore an arbitrary combination of axial forces, bending moments and shear forces, which can be isolated into nine basic load cases (see Fig. 25). By using these isolated load cases individually in parametric studies, the SNCF values for any arbitrary loading combination can be obtained from proportional summations of SNCFs from the basic load cases. However, because such an approach is not practical for parametric studies, a rationalized approach is preferred, where the boundary conditions and three load cases shown in Fig. 26 are chosen for the parametric study. The loading is such that unit nominal axial and bending strains are obtained for the respective axial and bending load cases.

10.2 *Implied effect of weld using a shift rule*

As discussed earlier, the weld shape and condition of the weld toe influences the SNCF close to the weld toe and is not included in evaluating the SNCF from the geometrical stress distribution. However, in most cases it is desirable to model the weld with solid elements, because the weld stiffness, attachment between the parent metal and weldment, as well as interpretation of results is straightforward and more correctly idealized. However, with K joints, because a large number of very small elements are necessary near the weld area, such joints could not be handled at the moment when the work was carried out, when modelling half of a K joint (using symmetry about the central in-plane axis of the joint). Parametric studies incorporating a quarter of a K joint could not be handled when using solid elements in the weld area because although geometrical symmetry can be applied, neither loading symmetry nor anti-symmetry is present.

An investigation is therefore carried out to determine how to model and interpret the output if the solid elements in the weld area are replaced by shell elements. A quarter of the K joint is modelled with two structural idealizations. Model 1 uses only shell elements and Model 2 is idealized in a similar manner to X and T joints, including shell, solid and transition elements in the weld area (Van Dooren et al. 1988). A comparison of the results of these two analyses would indicate a method of interpreting the results when half the K joint is modelled with only shell elements in the weld area as in Fig. 31. When modelling a quarter of the K joint, geometrical symmetry is present. However, loading antisymmetry, which is assumed for this model, is not strictly present (see Fig. 26). The difference from the boundary conditions in Fig. 26 is that both supports on the chord are implied to take up equal and antisymmetric reactions because of the assumed antisymmetrical boundary conditions in the central cross-section of the chord. The basic difference between Model 1 and Model 2 is sketched in Fig. 27, which could represent the cross-section of a weld region at the side of the joint. For Model 1, hot spot strains are obtained at the intersection between shell elements, while Model 2 gives hot spot strains at the properly modelled weld toe.

A comparison is carried out along the lines shown in Fig. 28, using quadratic extrapolation as discussed in chapter 7 and is satisfactory for dominant SNCF values (± 12% maximum). For lower SNCFs, where larger variations occur, they are mainly due to the difference in orientation of the principal strains between the results of the two models. It is concluded that FE models of K joints with gap of the type discussed here, where the weld and intersection area are modelled only with shell elements, should have their strain gradients shifted along brace or chord, as the case may be, from the intersection between the brace and chord elements to a position representing the centre of gravity of

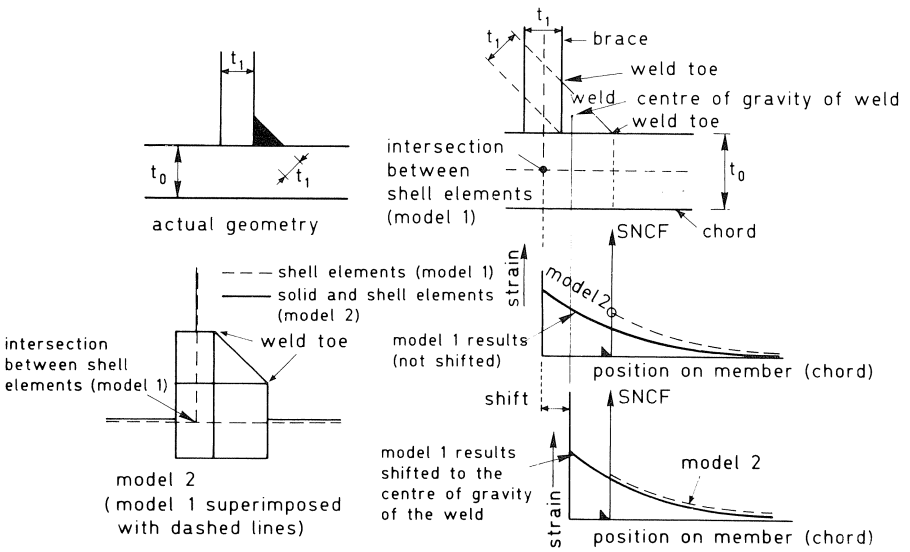

Fig. 27. Difference between model with and without welds for a location at the side of the K joint.

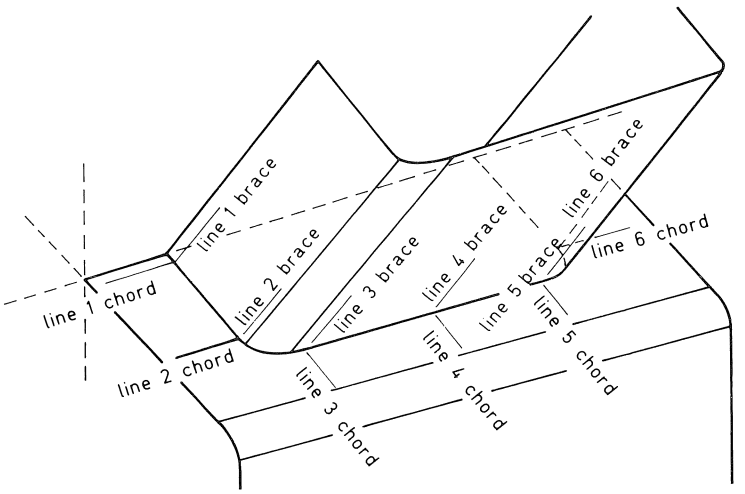

Fig. 28. Positions of strain lines in comparative study.

the weld (see Fig. 27). This gives an "average" representation of a model in which the weld area is modelled with shell, solid and transition elements. This shift rule is satisfactory for the SNCFs obtained for the governing values.
The modelling of the weld area and intersection of brace and chord only with shell elements, together with this shift rule, should only be used when the modelling of this area with a combination of shell, solid and transition elements cannot be carried out due to computational restrictions. It is always better to model the intersection of brace and chord with shell, solid and transition elements as in X and T joints, if possible. For the reasons mentioned above, the rest of the work on K joints with gap that is presented here is modelled with half of the K joint (see Fig. 31), with boundary conditions and load cases as shown in Fig. 26 and the brace/chord intersection modelled only in shell elements. The results are treated to the shift rule discussed in this chapter.

10.3 *Experimental comparison*

As mentioned before, the SNCF values are generally lower for K joints with gap than for X and T joints. Also, the strain distribution is not as strongly non-linear. Consequently, the SNCF values are not as sensitive to small variations of measured dimensions with respect to nominal dimensions, and the experimental measurements can be compared solely with the FE analysis using nominal dimensions of the hollow sections. The analysis using measured dimensions is therefore not carried out. Only one test is carried out and the parameters chosen for the experiment are $\beta = 0.6$, $2\gamma = 25$, $\tau = 0.5$ (chord = $200 \times 200 \times 8$ mm, braces = $120 \times 120 \times 4$ mm). The K joint specimen is shown during the static testing in Fig. 29. As mentioned before, no fatigue testing is carried out, as this is being done at Karlsruhe (Mang et al. 1988a, 1988d). Measurements of strains are

carried out using 87 strain gauges, some of which also measure the nominal strains on the various faces of the members so as to isolate the axial and bending strain contributions to the nominal strain. This is necessary, because the support conditions in the test rig are not the same as those assumed in Fig. 26. The left hand brace is supported by a hinged joint capable of axial movement. An axial compression is applied to this left hand brace by the hydraulic jack (see Fig. 29). The right hand brace has a long extension fixed to it, which is connected to the test rig by means of a hinged joint. The left hand support is attached to a cable which can apply tension to the chord at any desired eccentricity to the neutral axis of the chord. Only vertical displacement is therefore possible on the left hand support of the chord. The right hand end is free, as can be seen in Fig. 29.

Three loading situations are created by applying eccentricities to the cable of 0, $\frac{1}{4}b_0$ and $\frac{1}{2}b_0$ from the neutral axis vertically upwards up to the chord face. These eccentricities have a considerable influence on the bending moment magnitudes and therefore give a good range of proportions between bending and axial strains for the comparison with the FE analyses. Fig. 30 shows arrangement of strain gauges and lines along which comparisons have been made.

For the FE analyses, Fig. 31 shows the modelling chosen for the half K joint, where only shell elements are used in the weld and intersection area. This model is also chosen for the rest of the analyses in the parametric study. Since the nominal axial and bending

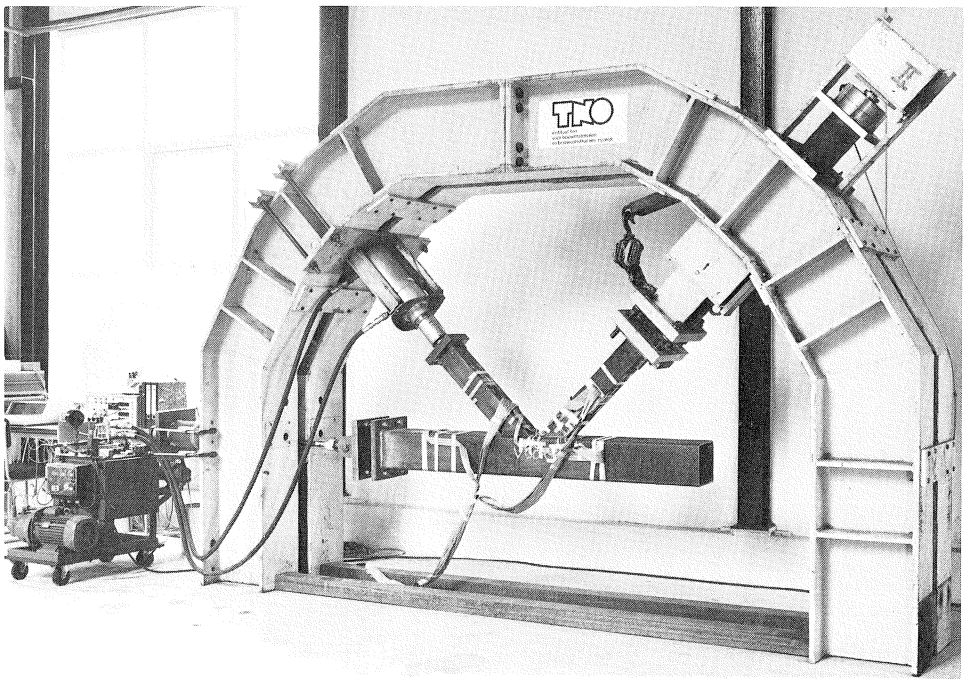

Fig. 29. Test set up for K joint with gap.

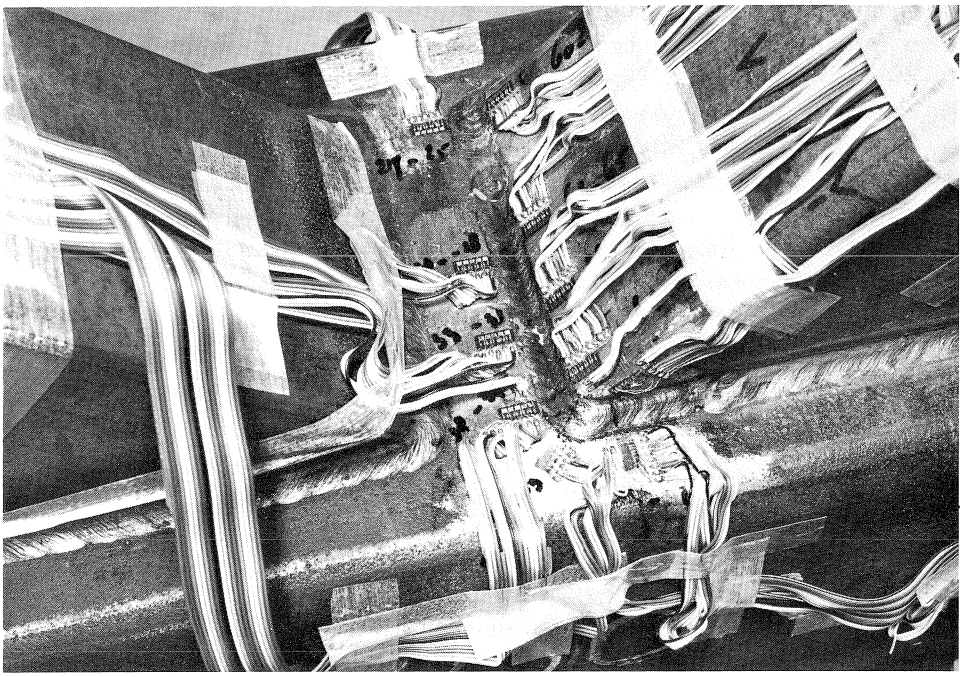

Fig. 30. Some strain gauge locations in the gap region of the K joint test specimen.

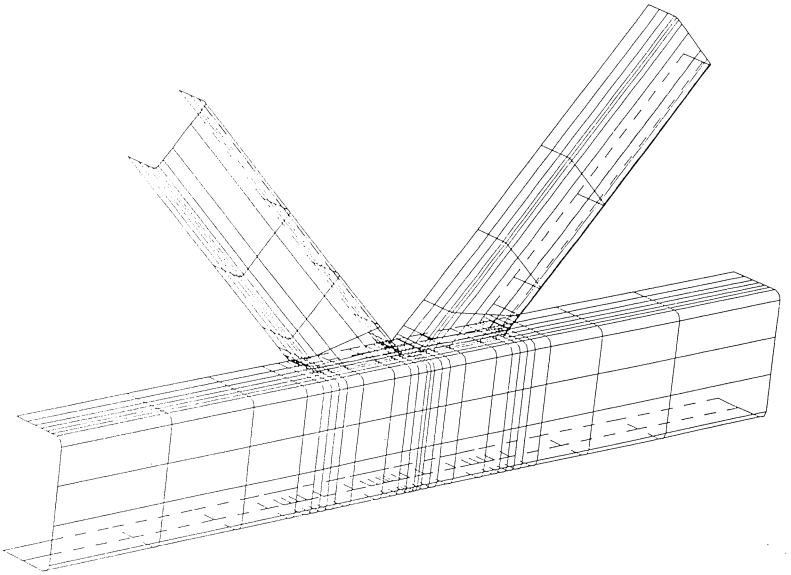

Fig. 31. Typical geometry of half of a K joint with gap used in the parametric study.

Table 5. Nominal dimensions of square hollow sections used in FE analyses of K joints with gap

$\beta = b_1/b_0$	$2\gamma = b_0/t_0 = 25$			$2\gamma = b_0/t_0 = 16$			$2\gamma = b_0/t_0 = 12.5$		
	chord	braces	no.	chord	braces	no.	chord	braces	no.
0.4	200 × 200 × 8	80 × 80 × 4	K1				200 × 200 × 16	80 × 80 × 4	K21
	200 × 200 × 8	80 × 80 × 4	K20				200 × 200 × 16	80 × 80 × 8	K2
0.6	200 × 200 × 8	120 × 120 × 4	K3				200 × 200 × 16	120 × 120 × 4	K22
				200 × 200 × 12.5	120 × 120 × 6.3	K24			
	200 × 200 × 8	120 × 120 × 8	K4				200 × 200 × 16	120 × 120 × 8	K5
							200 × 200 × 16	120 × 120 × 12.5	K23

strains are determined for the experiments, it is possible to add the correct proportions of nominal strains for the three load cases in Fig. 26 to simulate the three loading situations in the experiment. The shift rule is applied to interpret the results.
A comparison of SNCF values between experimental and numerical results using quadratic extrapolation (see chapter 7) is made and it is concluded that the dominant SNCF values for brace and chord from the FE analysis deviate up to ± 17% for the three eccentricities of loading for the experiment. This deviation can be accepted in view of the use of the shift rule. However, the use of solid elements would give more acceptable results. The higher variations for small SNCF values are mainly attributed to different orientations of principal strains between the experiment and the analysis using shell elements, in a similar manner as discussed in chapter 10.2.

10.4 *Parametric study using nominal dimensions of hollow sections*

Ten FE analyses have been carried out using the parametric variations given in Table 5. Only shell elements are used in the weld and brace/chord intersection area, where the shift rule is applied for interpreting results, as discussed in chapter 10.2.
Three load cases are used as discussed in chapter 10.1 and shown in Fig. 26, to investigate the influence of axial tension and bending in the braces. Since linear elastic behaviour is assumed, it is possible to describe the SNCF values for the whole range of nominal bending strain as a proportion of total strain from only two load combinations. One combination with only axial load and the other with the same proportions of bending moments and no axial load on the two braces. The SNCF values for three combinations are determined only along lines 2, 3, 5 and 6 shown in Fig. 28, where dominant SNCF

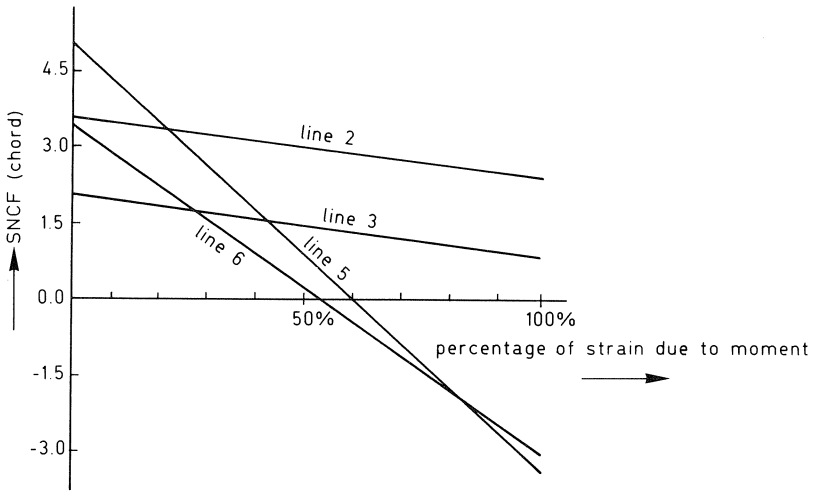

Fig. 32. Quadratically extrapolated SNCF values in chord of K joint with gap (joint K3) for various proportions of brace moments.

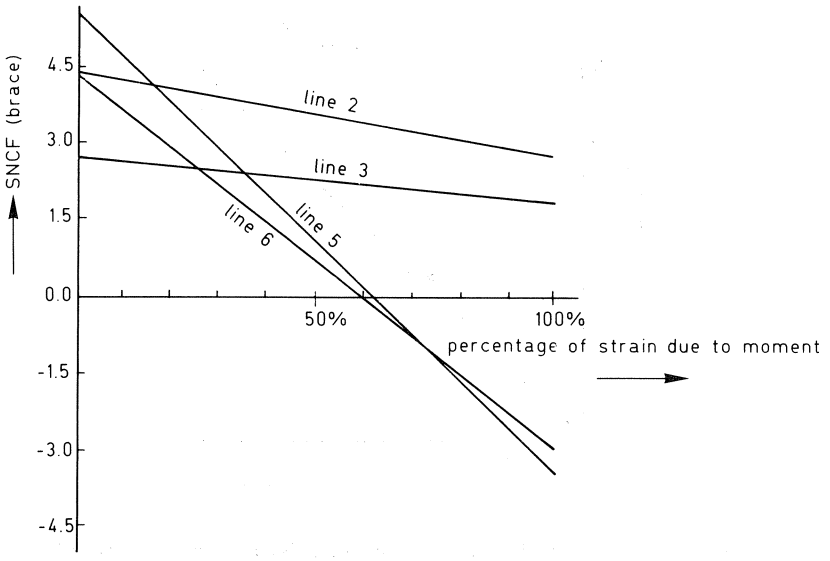

Fig. 33. Quadratically extrapolated SNCF values in brace of K joint with gap (joint K3) for various proportions of brace moments.

values are present. Only quadratically extrapolated values are presented. The results of this work are provided in the form of graphs as shown typically for joint K3 in Figs. 32 an 33. It is found from observations of such plots for all the K joints considered, that for moment percentages above 15 to 20%, line 2 in the brace and chord gives the highest SNCF values. Also, there is no large variation of SNCF values for line 2 with different moment percentages. Therefore, as long as the moment percentage in practical cases is above 20%, the governing SNCF values lie in the gap region and there is also no large change in the SNCF values with variations in moment.

For the parametric study, however, SNCF values are taken from the plots shown typically in Figs. 32 and 33 at moment percentages where the nominal bending strain is 33% of the maximum algebraic sum of nominal axial and bending strain. This is because in the recommended fatigue rules of the IIW subcommittee XV E (1982), a multiplication factor of 1.5 is used on the axial stresses of joints where the bending moment is unknown. For this proportion, the maximum SNCF values for all the analyses are on line 2 in the chord and brace (see Fig. 28).

A stepwise regression analysis is carried out to determine the SNCF formulae given below for moment contribution of 33%. Only results for quadratic extrapolation (see chapter 7) are presented.

$$\mathrm{SNCF}^{33\%}_{\mathrm{chord}} = (2.84 - 3.1\beta)\left(\frac{2\gamma}{12.5}\right)^{(1.02+1.1\beta)}\left(\frac{\tau}{0.5}\right)^{(0.8+0.5\beta)}$$

$$\mathrm{SNCF}^{33\%}_{\mathrm{brace}} = 1.0 + (1.49 - 0.9\beta)\left(\frac{2\gamma}{12.5}\right)^{(3.13-2.55\beta)}\left(\frac{\tau}{0.5}\right)^{(-0.25+1.5\beta)}$$

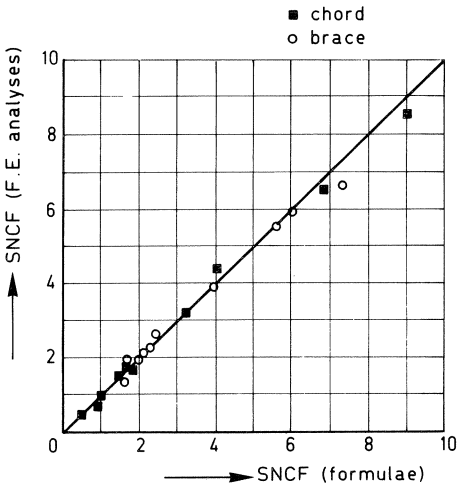

Fig. 34. Comparison between quadratically extrapolated SNCFs from analyses and formulae for K joints with gap.

The validity range for these formulae is:

$$\begin{aligned} 0.4 &\leq \beta \leq 0.6 \\ 12.5 &\leq 2\gamma \leq 25 \\ 0.25 &\leq \tau \leq 1.0 \\ e &= 0 \end{aligned}$$

For other moment percentages, the following formula is determined:

$$\mathrm{SNCF}^{M\%} = \left[1.13 - 0.4\left(\frac{f_b}{f_a + f_b}\right)\right] \mathrm{SNCF}^{33\%}$$

In Fig. 34, a comparison between the SNCFs from the formulae and those from the numerical analyses for line 2 in the brace and chord is given. As can be seen, the agreement is good. In Fig. 35, the SNCF values are given graphically in order to give an impression of the SNCF values and dependence of various parameters. It is emphasised that the gap function is implicitly included in the β dependence for the SNCF formulae (for zero eccentricity of system lines).

Also, the SNCF formulae presented in the parametric study may be described as qualitative. This work and the work to be carried out on K joints with overlap will be used together with the work at Karlsruhe (Mang et al. 1988a, 1988b, 1988c, 1988d) to present more detailed information. Further adjustments to the formulae due to regression analysis on more data points are also likely.

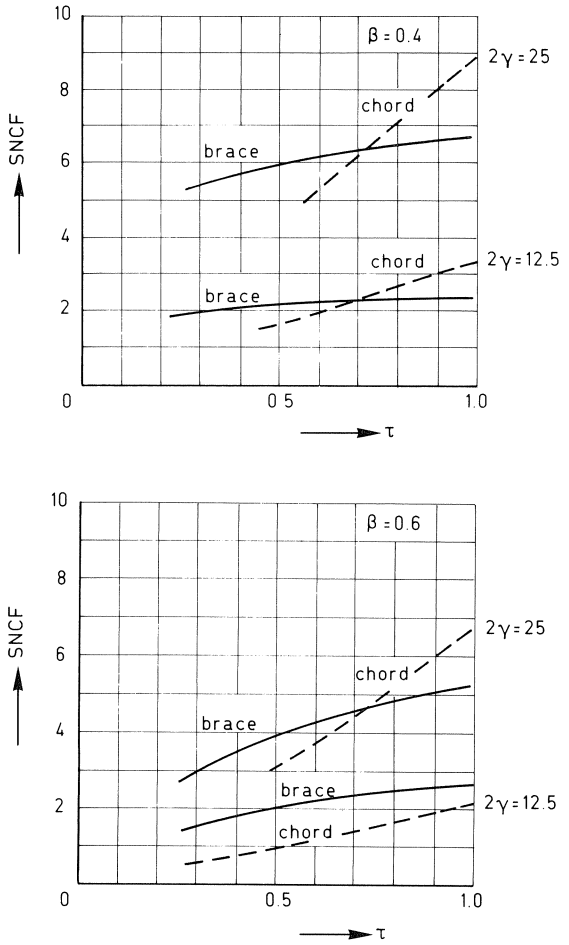

Fig. 35. Relationship between the ratio $\tau = t_1/t_0$ and the quadratically extrapolated SNCF values from formulae for K joints with gap (and no eccentricity of system lines).

11 Concluding remarks

This article discusses numerical (FE) modelling and experimental testing on X and T joints and K joints with gap, using square hollow sections, to obtain strain concentration factors. This SNCF data can be used in predicting the fatigue behaviour of such joints. Therefore, only background information on fatigue design is given.

FE analyses have been carried out for a range of parametric variations using the nominal dimensions of a selected size of joint. The work reported here is based mainly upon chord widths of 200 mm. Simple rectangular FE meshes have been used where possible, so that data generation even with sophisticated preprocessors is rapidly obtained for the large number of joints to be considered in parametric studies.

Two strain extrapolation methods (linear and quadratic) have been illustrated, which are used to determine SNCF values from the results of each FE analysis. Using these values, SNCF formulae are presented for each joint type at critical locations for selected loading situations. These have been obtained from regression analyses, valid within the range of parameters investigated. The SNCF formulae are based upon non-dimensional geometrical parameters β, 2γ and τ.

The modelling of the weld and intersection of the chord and braces with shell, solid and transition finite elements is shown, together with the ease and accuracy of interpreting the results. This method is particularly desirable for large and strongly non-linear strain gradients. Where it is not possible to follow this approach due to computational limitations, a "shift rule" is proposed for interpreting the results and a computationally less demanding model having only shell elements in this region is used.

Test specimen sizes for measuring strains from linear static tests, which are used for checking the FE model results, are selected for fabrication from representative joints having the same nominal sizes of members as in the parametric study. The results of these tests compare well with FE analyses using measured dimensions of the test specimens. When analyses with nominal dimensions of the hollow sections have been carried out, the results differ from experimental values because of the variations between nominal and measured dimensions. These variations appear to increase with decreasing joint size.

X, T and K joints have been treated separately in this article. It is intended to include the results of all the work on X, T and K joints (K joints with gap and with overlap) in a unified approach where, for instance, the extrapolation method, influence of weld type (fillet or butt weld), factors for dimensional tolerances and factors for conversion of strain concentration factors (SNCF) into stress concentration factors (SCF) are taken jointly into account. The SNCF formulae that are eventually established will be presented in graphical form for practical use, where the influence of the non-dimensional parameters on SNCF magnitudes can be visually observed.

It is proven from hands on experience that large scale parametric studies for establishing strain (stress) concentration factors (SNCF) and parametric SNCF formulae from FE analyses on joints in hollow sections are practicable in an environment with minicomputers.

12 Acknowledgements

The donation by "van Leeuwen Buizen", Zwijndrecht and "Oving-Diepeveen-Struycken B.V.", Barendrecht of the hollow sections used for the test specimens in this programme, and the financial support of the "Staalbouwkundig Genootschap" is gratefully acknowledged. The authors wish to express their appreciation of the permission given by ECSC and CIDECT to publish this work. The interim reports on "Fatigue behaviour of joints between rectangular hollow sections" are confidential until final approval by the ECSC.

The authors also wish to thank their colleagues in the respective Steel Departments for

their support. Important contributions in the successful completion of different stages of the project are given by the following persons:
At IBBC-TNO, Ir. H. M. G. M. Steenbergen for his assistance with computer runs and particularly modelling with PATRAN. Also Mr. K. C. A. Jungschlager (Chief Technician) for his supervision of experiments and assistance with computer runs and output interpretation. Transition finite elements that are necessary for compatibility at the junction between shell and solid elements have been implemented into the general purpose computer program DIANA by Mr. P. Nauta.
At Delft University of Technology, Mr. A. Verheul for his experimental work on T joints.

13 References

AHMAD, S., B. M. IRONS and O. C. ZIENKIEWICZ (1970), Analysis of thick and thin shell structures by curved finite elements, International Journal for Numerical Methods in Engineering, Vol. 2, 419–451.

BREBBIA, C. (1982), Editor, Finite Element Systems – A Handbook, second Edition, Springer-Verlag, Berlin, Heidelberg, New York.

DE BORST, R., G. M. A. KUSTERS, P. NAUTA and F. C. DE WITTE (1985), DIANA – A comprehensive but flexible finite element system, Finite Element Systems Handbook, Editor C. A. Brebbia, Springer-Verlag, Berlin.

DE KONING, C. H. M., R. S. PUTHLI, J. WARDENIER and D. DUTTA (1988), Fatigue behaviour of joints between rectangular hollow sections – X joints, Part 4, Analyses, conclusions and suggested recommendations from work on X joints in R.H.S., with brace in tension. TNO-IBBC Report no. BI-88-039, TU-Delft, Stevin report 6-88-5, M and C 25-88-11, Revision 1, March 1988.

EFTHYMIOU, M. and S. DURKIN (1985), Stress concentrations in T/Y and gap/overlap joints, Behaviour of Offshore Structures (BOSS), Edited by J. A. Battjes, Elsevier Science Publishers, B.V., Paper B 11, 429–440.

GIBSTEIN, M. B. (1978), Parametric stress analysis of T-joints, Seminar of the European Coal and Steel Community, Cambridge, November 1978.

International Institute of Welding, IIW-XV-E (1985), Recommended fatigue design procedure for hollow section joints Part 1, Hot spot stress method for nodal joints, IIW Doc. XV-582-85/ XIII-1158-85.

KUANG, J. G., A. B. POTVIN, R. D. LEICK and J. L. KAHLIC (1977), Stress concentration in tubular joints, SPE Journal, August edition 1977.

MANG, F., S. HERION, J. KLINGER, O. BUCÄK and D. DUTTA (1988a), Zeit- und Dauerfestigkeit von geschweissten unversteiften Rechteck – Hohlprofilverbindungen von Fachwerken und Vierendeelträgern – K Knoten, Teil 1: Experimentelle Untersuchungen und Dauerfestigkeit unter axialer Belastung der Diagonalen, Bericht, Universität Karlsruhe (TH), Revision 1, February 1988.

MANG, F., S. HERION, J. KLINGER, O. BUCÄK and D. DUTTA (1988b),Zeit- und Dauerfestigkeit von geschweissten unversteiften Rechteck – Hohlprofilverbindungen von Fachwerken und Vierendeelträgern – K Knoten, mit Spalt, Teil 2: Berechnungen nach der Methode der Finiten Elemente und Vergleich mit den Versuchsergebnissen zur Bestimmung von Dehnungskonzentrationsfaktoren, Bericht, Universität Karlsruhe (TH), revision 1, January 1988.

MANG, F., S. HERION, J. KLINGER, O. BUCÄK and D. DUTTA (1988c), Zeit- und Dauerfestigkeit von geschweissten unversteiften Rechteck – Hohlprofilverbindungen von Fachwerken und Vierendeelträgern – K Knoten, mit Spalt, Teil 3: Bestimmung von Dehnungskonzentrationsfaktoren und ihr Einfluss auf die Dauerfestigkeit, Bericht, Universität Karlsruhe (TH), February 1988.

MANG, F., S. HERION, J. KLINGER, O. BUCÄK and D. DUTTA (1988d), Zeit- und Dauerfestigkeit von geschweissten unversteiften Rechteck - Hohlprofilverbindungen von Fachwerken und Vierendeelträgern - K Knoten, überlappt, Teil 1: Experimentelle Untersuchungen und Dauerfestigkeit unter axialer Belastung der Diagonalen, Bericht, Universität Karlsruhe (TH), March 1988.

PUTHLI, R. S. (1981), Geometrical non-linearity in collapse analysis of thick walled shells, with application to tubular steel joints, HERON, Volume 26, No. 2.

PUTHLI, R. S., C. H. M. DE KONING, J. WARDENIER and D. DUTTA (1986), A study on strain concentration factors of square hollow section X joints with brace in tension, TNO-IBBC Report no. BI-86-63, TU-Delft Stevin Report no. 6-86-7.

PUTHLI, R. S., C. H. M. DE KONING, J. WARDENIER and D. DUTTA (1988), The fatigue behaviour of X joints made from square hollow sections, Paper 3, Weldtech 88 - International Conference on Weld Failures, London, U.K., November, 22-25, 1988.

VAN DELFT, D. R. V., C. NOORDHOEK and J. DE BACK (1985), Evaluation of the European fatigue test data on large-size welded tubular joints for offshore structures, OTC paper 4999, Houston, Texas, May 1985.

VAN DELFT, D. R. V., C. NOORDHOEK and M. L. DA RE (1987), The results of the European fatigue tests on welded tubular joints compared with SCF formulas and design lines, Steel in Marine Structures, edited by C. Noordhoek and J. de Back, Elsevier Science Publishers, B.V., Amsterdam, Paper TS 24, 565-577.

VAN DOOREN, F. J., R. S. PUTHLI and J. WARDENIER (1988), Fatigue behaviour of joints between rectangular hollow sections - Numerical determination of strain concentration factors of K gap joints made of rectangular hollow sections, TNO-IBBC report no. BI-88-074, TU-Delft Stevin Report 6-88-9, M and C 25-88-29, May 1988.

VAN WINGERDE, A. M., A. VERHEUL, R. S. PUTHLI, J. WARDENIER and D. DUTTA (1988), The fatigue behaviour of T joints made of square hollow sections, Paper 4, Weldtech 88 - International Conference on Weld Failures, London, U.K., November 22-25, 1988.

WARDENIER, J. (1982), Hollow Section Joints, First edition, Delft University Press, Delft, The Netherlands.

WORDSWORTH, A. C. (1981), Stress concentration factors at K and KT tubular joints, Conference on Fatigue in Offshore Structural Steels, Institution of Civil Engineers, London, February 1981.

WORDSWORTH, A. C. (1987), Aspects of the stress concentration factors at tubular joints, Steel in Marine Structures, edited by C. Noordhoek and J. de Back, Elsevier Science Publishers B.V., Amsterdam, paper TS8, 349-361.